0830-L-02 NAS 1.29/3:00-09

NASA Tech Briefs

National Aeronautics and Space Administration

Electronic Components and Circuits

Electronic Systems

Physical Sciences

Materials

Computer Programs

Mechanics

Machinery

Fabrication Technology

Mathematics and Information Sciences

Life Sciences

20020255374 C

INTRODUCTION

Tech Briefs are short announcements of innovations originating from research and development activities of the National Aeronautics and Space Administration. They emphasize information considered likely to be transferable across industrial, regional, or disciplinary lines and are issued to encourage commercial application.

Availability of NASA Tech Briefs and TSPs

Requests for individual Tech Briefs or for Technical Support Packages (TSPs) announced herein should be addressed to

National Technology Transfer Center
Telephone No. **(800) 678-6882** or via World Wide Web at **www2.nttc.edu/leads/**

Please reference the control numbers appearing at the end of each Tech Brief. Information on NASA's Commercial Technology Team, its documents, and services is also available at the same facility or on the World Wide Web at **www.nctn.hq.nasa.gov**.

Commercial Technology Offices and Patent Counsels are located at NASA field centers to provide technology-transfer access to industrial users. Inquiries can be made by contacting NASA field centers and program offices listed below.

NASA Field Centers and Program Offices

Ames Research Center
Carolina Blake
(650) 604-1754 or
cblake@mail.arc.nasa.gov

Dryden Flight Research Center
Lee Duke
(805) 258-3802 or
lee.duke@dfrc.nasa.gov

Goddard Space Flight Center
George Alcorn
(301) 286-5810 or
galcorn@gsfc.nasa.gov

Jet Propulsion Laboratory
Merle McKenzie
(818) 354-2577 or
merle.mckenzie@jpl.nasa.gov

Johnson Space Center
Hank Davis
(281) 483-0474 or
henry.l.davis1@jsc.nasa.gov

John F. Kennedy Space Center
Gale Allen
(407) 867-5226 or
gale.allen-1@ksc.nasa.gov

Langley Research Center
Sam Morello
(757) 864-6005 or
s.a.morello@larc.nasa.gov

Glenn Research Center
Larry Viterna
(216) 433-3484 or
cto@grc.nasa.gov

George C. Marshall Space Flight Center
Sally Little
(256) 544-4266 or
sally.little@msfc.nasa.gov

John C. Stennis Space Center
Kirk Sharp
(228) 688-1929 or
technology@ssc.nasa.gov

NASA Program Offices
At NASA Headquarters there are seven major program offices that develop and oversee technology projects of potential interest to industry:

Carl Ray
Small Business Innovation Research Program (SBIR) & Small Business Technology Transfer Program (STTR)
(202) 358-4652 or
cray@mail.hq.nasa.gov

Dr. Robert Norwood
Office of Commercial Technology (Code RW)
(202) 358-2320 or
rnorwood@mail.hq.nasa.gov

John Mankins
Office of Space Flight (Code MP)
(202) 358-4659 or
jmankins@mail.hq.nasa.gov

Terry Hertz
Office of Aero-Space Technology (Code RS)
(202) 358-4636 or
thertz@mail.hq.nasa.gov

Glen Mucklow
Office of Space Sciences (Code SM)
(202) 358-2235 or
gmucklow@mail.hq.nasa.gov

Roger Crouch
Office of Microgravity Science Applications (Code U)
(202) 358-0689 or
rcrouch@hq.nasa.gov

Granville Paules
Office of Mission to Planet Earth (Code Y)
(202) 358-0706 or
gpaules@mtpe.hq.nasa.gov

NASA TechBriefs
National Aeronautics and Space Administration
September 2000
00-09

5 Electronic Components and Circuits

11 Electronic Systems

17 Physical Sciences

27 Materials

33 Computer Programs

37 Mechanics

41 Machinery

47 Fabrication Technology

51 Mathematics and Information Sciences

57 Life Sciences

This document was prepared under the sponsorship of the National Aeronautics and Space Administration. Neither the United States Government nor any person acting on behalf of the United States Government assumes any liability resulting from the use of the information contained in this document, or warrants that such use will be free from privately owned rights.

4

BLANK PAGE

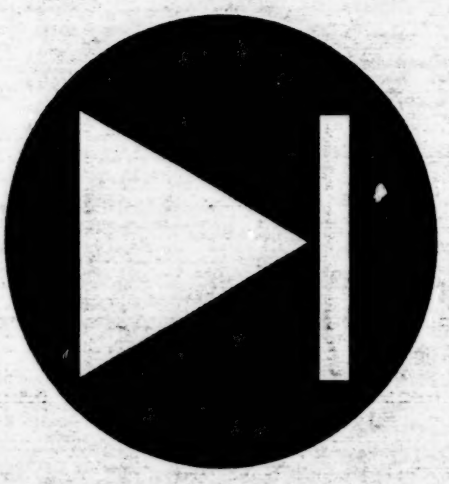

Electronic Components and Circuits

Hardware, Techniques, and Processes

7 CMOS APS With Integrated Centroid-Computation Circuits
7 Parallel Integrated Frame Synchronizer Chip
9 An Electro-Optical Frequency Shifter

BLANK PAGE

CMOS APS With Integrated Centroid-Computation Circuits

Power consumption, latency, and size can be reduced.

NASA's Jet Propulsion Laboratory, Pasadena, California

An advanced complementary metal oxide/semiconductor (CMOS) active-pixel sensor (APS) incorporates integrated circuitry that computes the centroid of the image in a window selectable by the user. The development of this circuitry is significant in that it is necessary to compute centroids of images in diverse applications that include robotic vision, autonomous navigation, optical communications, and scientific imaging. Heretofore, it has been necessary to compute centroids by use of off-chip circuitry, at the cost of increased data latency, power consumption, and system size. This circuitry computes image centroids on-chip at a high speed and in analog domain, while consuming little additional power, and is compatible with high-performance CMOS APS circuitry.

The prototype window-centroiding CMOS APS contains a 128 × 128-pixel APS with its readout circuitry, plus the centroid processor, which includes a switching network, analog inner-product (IP)-computing circuits, and an analog divider (see figure). The centroid computer operates on a window of $n \times n$ pixels, where $3 \leq n \leq 9$ to produce both x and y centroids. Computation of the centroid involves the computation of inner products (weighted sums) and division of the weighted sums by an overall nonweighted sum. Each term in each inner product is proportional to a pixel voltage (which is nominally proportional to pixel brightness) weighted by the integer (between 1 and n, inclusive) that represents the pixel row (y) or column (x) address within the window.

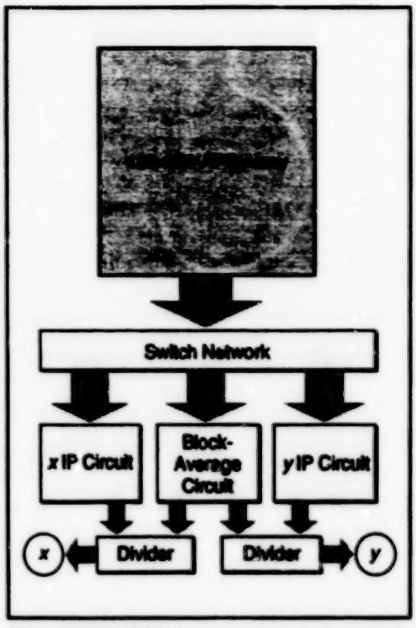

This **CMOS APS** incorporates high-speed, on-chip circuits that compute the centroid of the image in $n \times n$ window.

The inner products are computed in the following way: Timed electronic switches are used to sample the pixel voltages to separate sampling capacitors, the sizes of which are proportional to the integer row and column addresses. The row and column inner products are obtained by simultaneously dumping the charges on the corresponding sampling capacitors into analog charge-summing circuits. Finally, by use of a single divider circuit, the row and column inner products are divided by scale factors proportional to the nonweighted sum of pixel voltages in the window to obtain the x and y centroid values. These computations are performed in column-parallel fashion, so that centroids are computed at the row-readout rate, enabling high-speed, low-power centroid computation.

In tests, centroid errors were determined for various image brightnesses and various sizes and locations of windows; the errors were found to range from about 0.02 pixel over most of the APS array to a worst-case value of about 0.07 pixel for a 3 × 3 window. Overall, the results of the tests were interpreted as signifying that one can determine centroids to within 0.05 pixel under most lighting conditions while operating at the update rates used in the tests (20 to 50 kHz).

This work was done by Bedabrata Pain, Chao Sun, and Guang Yang of Caltech for **NASA's Jet Propulsion Laboratory.** *Further information is contained in a TSP [see page 1].*

In accordance with Public Law 96-517, the contractor has elected to retain title to this invention. Inquiries concerning rights for its commercial use should be addressed to

Technology Reporting Office
JPL
Mail Stop 122-116
4800 Oak Grove Drive
Pasadena, CA 91109
(818) 354-2240

Refer to NPO-20715, volume and number of this NASA Tech Briefs *issue, and the page number.*

Parallel Integrated Frame Synchronizer Chip

This chip can handle data in a variety of formats at rates up to 500 Mb/s.

Goddard Space Flight Center, Greenbelt, Maryland

The Parallel Integrated Frame Synchronizer (PIFS) chip is one of three very-large-scale integrated (VLSI) circuits designed for ground processing of streams of telemetric data received from spacecraft. These application-specific integrated circuits (ASICs) are the main components of a developmental advanced telemetric-data-processing system that is intended to be smaller, cheaper, and more capable than its predecessors. Each of these ASICs is intended to perform most of the functions heretofore performed by multiple integrated circuits on printed-circuit cards. These ASICs are designed mainly to accommodate the packet-telemetry-data protocols recommended by the Consultative Committee for Space Data Systems (CCSDS); however, they also have generic capabilities in that they are programmable and can therefore also be made to handle telemetry in special data formats.

The three ASICs are used in return-link processing, which is the digital processing that takes place after the reception, demodulation, and digitization of signals transmitted from spacecraft. The return-link processing functions are apportioned sequentially among the three ASICs as follows:

1. The PIFS chip delineates frames of data from the incoming serial bit stream by implementing a sophisticated algorithm that searches for frame synchronizers, which are prescribed bit sequences placed at the frame boundaries.
2. The output of the PIFS chip is fed to the second ASIC, which is the Reed-Solomon Error Correction (RSEC) chip.

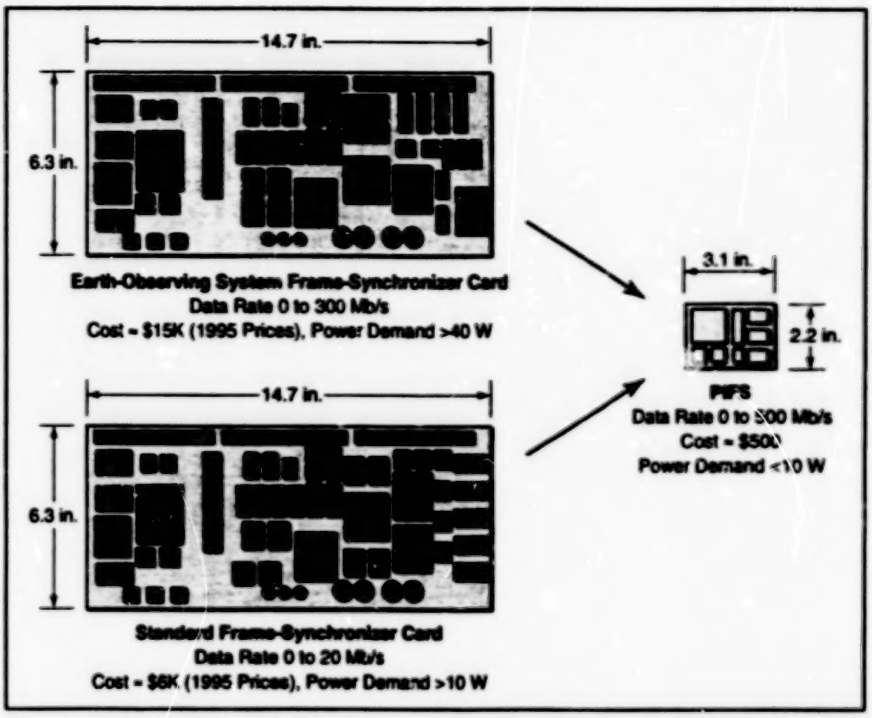

Figure 1. In Comparison with Prior Frame-synchronizer Circuitry, the PIFS chip is smaller, cheaper, and more capable.

For powerful protection against errors that can enter both the data and the protocol structures, the data frames are Reed-Solomon encoded, with interleaving, prior to transmission from the spacecraft. The RSEC decodes and de-interleaves the data and corrects any Reed-Solomon-correctable errors.

3. The output of the RSEC chip is fed to the third ASIC, which is the CCSDS Service Processor chip. This chip demultiplexes, extracts, and validates user data from the composite stream of telemetry frames.

The PIFS chip is a complementary metal oxide/semiconductor (CMOS) gate array laid out according to 0.6-μm design rules. As its name indicates, the PIFS chip implements a parallel-processing algorithm for synchronization of telemetry frames. Parallel processing requires logic circuitry significantly more complex than that required for serial processing; however, because advances in VLSI have greatly reduced the costs and sizes of logic circuits, the greater complexity of

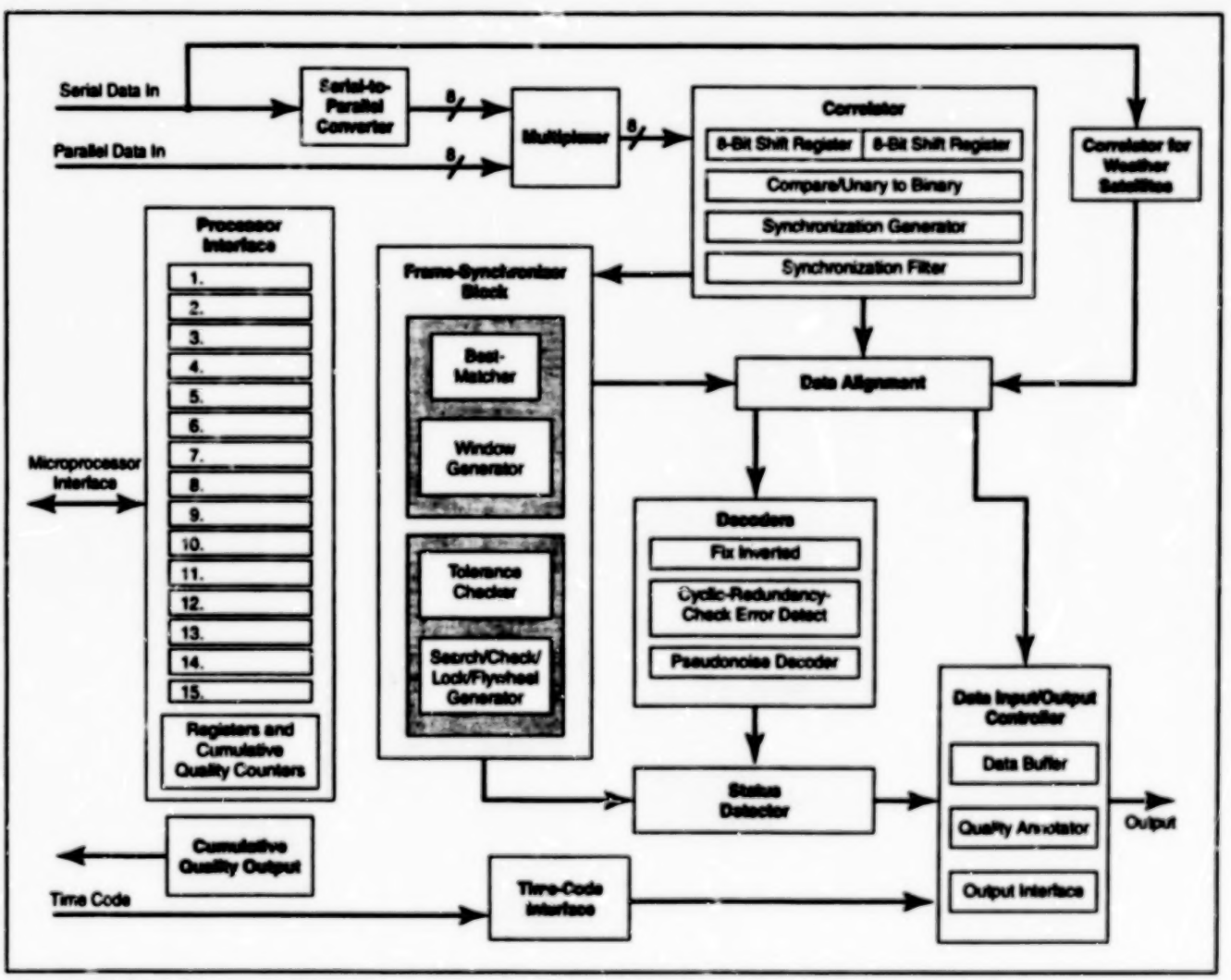

Figure 2. This Block Diagram depicts the flows of data and the major data-processing functional subdivisions of the PIFS.

the PIFS design is no longer a disadvantage. As shown in Figure 1, the PIFS chip is much smaller than two older multiple-VLSI-chip serial-processing frame synchronizers that it is intended to replace.

The PIFS chip is controlled by a set of internal registers that are configured through a standard microprocessor interface (see Figure 2) prior to operation. The registers afford the programmability that enables the PIFS to satisfy the frame-synchronization requirements of many different spacecraft missions. During operation, data enter the chip in one of two ways:

- If the data rate is very high, the serial data stream is first externally converted to a byte-wide parallel data stream and then fed into an internal first-in/first-out (FIFO) memory.
- If the data rate is <50 Mb/s, the serial data stream can be fed directly to the PIFS and converted to parallel internally.

The FIFO memory enables the logic circuitry within the PIFS to be synchronized with a separate master clock; this feature, in combination with a data-flow architecture, offers several advantages over older frame synchronizers, including lower latency, easier processing of nested or asynchronously blocked data, and automatic pipeline flushing. As data pass through the chip, correlations are computed, locations of synchronizers are calculated, and data are aligned to frame boundaries. The PIFS chip performs a superset of the functions of prior frame synchronizers, including cumulative quality accounting, time stamping, real-time quality trailer generation, and capability to synchronize all current weather-satellite formats. One exception is reverse data handling, which is expected to become unnecessary because of the planned ubiquitous use of solid-state recorders aboard spacecraft.

This work was done by Parminder S. Ghuman and Toby Bennett of **Goddard Space Flight Center** *and Jeff Solomon formerly of RMS Technologies. Further information is contained in a TSP [see page 1].*

This invention is owned by NASA, and a patent application has been filed. Inquiries concerning nonexclusive or exclusive license for its commercial development should be addressed to the Patent Counsel, Goddard Space Flight Center [see page 1]. Refer to GSC-13813.

An Electro-Optical Frequency Shifter

Frequency of a laser beam would be shifted up or down by as much as several gigahertz.

NASA's Jet Propulsion Laboratory, Pasadena, California

A proposed electro-optical apparatus would shift the frequency of a laser beam by a controllable amount within the range of about ±10 GHz. It would be a wide-band alternative to an acousto-optical tunable filter, which is limited to a frequency shift of about 100 kHz. The power efficiency of the proposed apparatus would be nearly 100 percent; the main insertion loss would be only about 2 dB and would be associated with fiber-optic input and output.

The apparatus would produce a constant frequency shift by exploiting the phase shift of the laser beam in an electro-optical medium. The effect, upon frequency, of a steadily increasing or decreasing phase shift is equivalent to the Doppler frequency shift produced by a steadily advancing or retreating mirror. Of course, there is no practical way to realize, in a compact apparatus, a steadily advancing or retreating mirror. Similarly, there is no practical way to realize its functional equivalent in a phase modulator in which the phase shift could be made to increase or decrease steadily without limit.

However, it is possible to drive two electro-optical modulators with identical sawtooth waveforms that differ in phase by about 180°. It is also possible to switch a laser beam electro-optically so that it repeatedly passes through one modulator and then the other. If this switching were done in proper synchronization with the sawtooth modulation waveform, then laser beam could be made to undergo either an increasing or a decreasing phase shift at all times. The proposed apparatus is based on this concept.

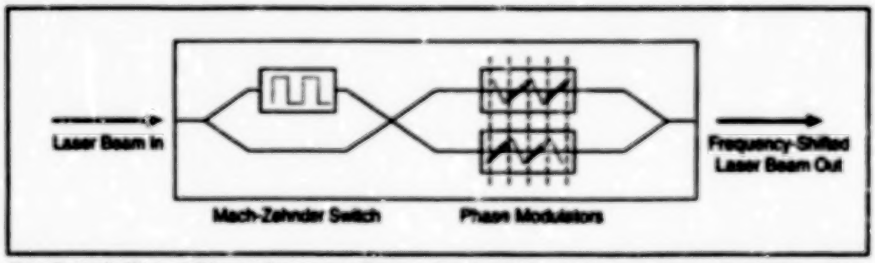

The Switch Would Direct the Laser Beam alternately through one phase modulator, then the other. The rectangular switching waveform would be synchronized so that at any given instant of time, the laser beam would be exposed to the rising edge (only) of the sawtooth modulating waveform.

The apparatus (see figure) would be made from standard lithium niobate integrated optics. A Mach-Zehnder switch driven by a rectangular waveform synchronized with the sawtooth modulating waveform would direct the laser beam alternately along optical paths to two phase modulators. The amplitude of the sawtooth waveform would typically be chosen to obtain a peak-to-peak phase modulation of 4π radians. The shift in frequency of the laser beam would equal the phase-modulation rate, which would be proportional to the amplitude and repetition frequency of the sawtooth waveform; for example, at a typical repetition frequency of 1 GHz, the frequency shift would be about 2 GHz.

The amplitude and phase relationships between the two sawtooth modulating waveforms would be chosen so that during the brief switching intervals in which parts of the laser power were passing partly through both phase modulators, the difference between the phase shifts produced by the two modulators would be 2π radians. This choice would ensure coherent addition of the outputs of the two modulators and prevent the introduction of a spurious phase modulation associated with the switching.

This work was done by Roman C. Gutierrez of Caltech for **NASA's Jet Propulsion Laboratory.** *Further information is contained in a TSP [see page 1].*

In accordance with Public Law 96-517, the contractor has elected to retain title to this invention. Inquiries concerning rights for its commercial use should be addressed to

Technology Reporting Office
JPL
Mail Stop 122-116
4800 Oak Grove Drive
Pasadena, CA 91109
(818) 354-2240

Refer to NPO-20531, volume and number of this NASA Tech Briefs issue, and the page number.

BLANK PAGE

Electronic Systems

Hardware, Techniques, and Processes

13 Airborne Multichannel Swept-Tuned Spectrum Analyzer
14 System Computes Flow Quantities From Acoustic-Sensor Output
15 Improved Eye-Tracking Apparatus
16 Improved Optical Fallout Monitor

BLANK PAGE

Airborne Multichannel Swept-Tuned Spectrum Analyzer

Dynamic data are transmitted in real time despite limited telemetry bandwidth.

Dryden Flight Research Center, Edwards, California

Two airborne spectrum analyzers were developed for acquiring dynamic data, characterized by frequencies up to 25 kHz, from a hypersonic-cross-flow-transition experiment aboard the air-launched Pegasus® space booster rocket (see Figure 1). Real-time transmission of time histories of the dynamic data via a pulse-code modulation (PCM) telemetry encoder would have required sample rates of at least 50,000 s^{-1}. The telemetry bandwidth necessary to sup-

Figure 1. The Pegasus® Air-Launched Space Booster Rocket is shown here at ignition of its engine after being dropped from a carrier aircraft. (NASA photo by Jim Ross.)

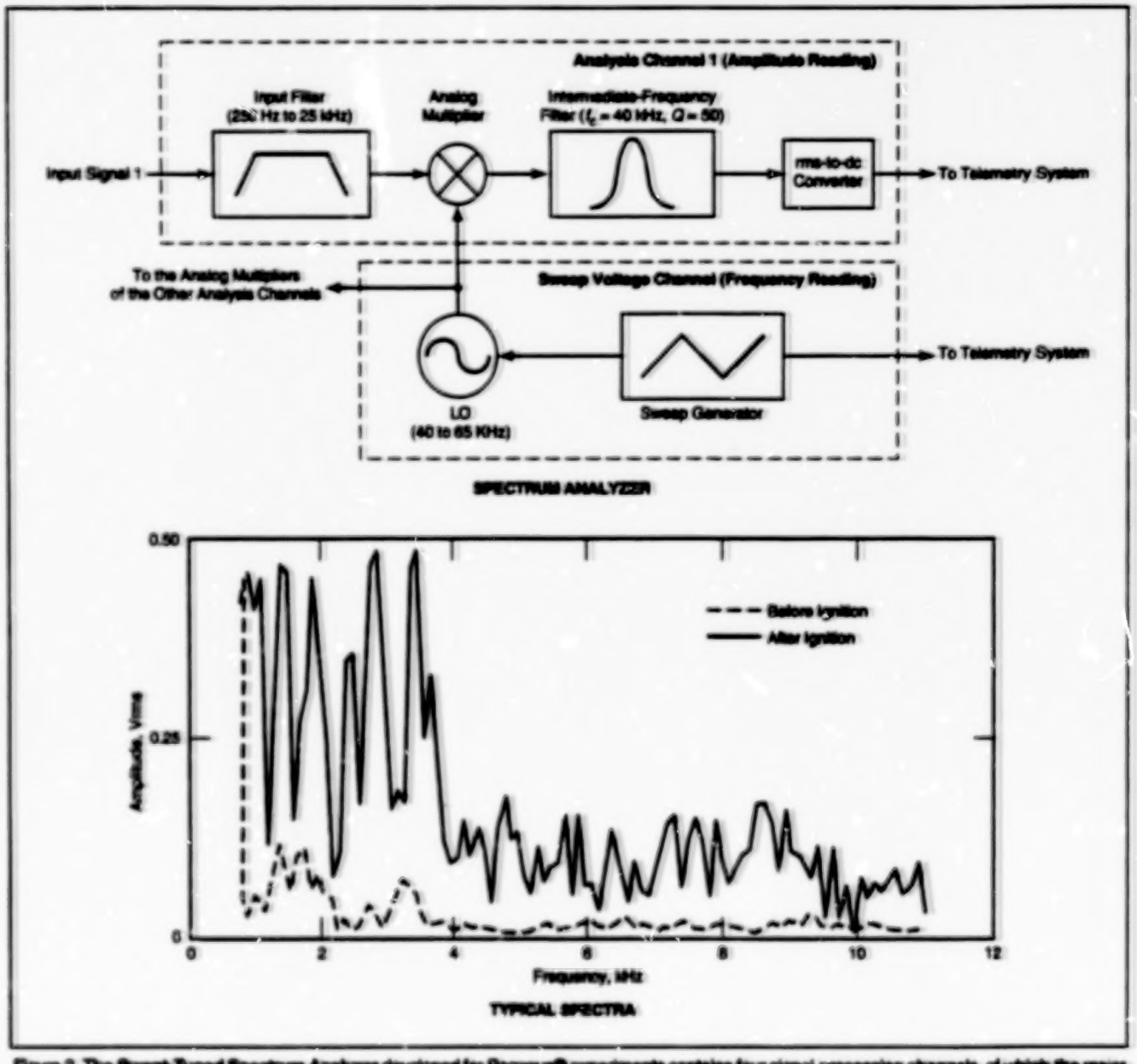

Figure 2. The Swept-Tuned Spectrum Analyzer developed for Pegasus® experiments contains four signal-processing channels, of which the major functional blocks are depicted here. The plots at the bottom are spectra obtained with the help of the swept-tuned spectrum analyzer.

port rates as high as this was not available; however, conversion of the data to the frequency domain aboard the rocket would make it possible to trade frequency resolution for a reduction in telemetry bandwidth. The two airborne spectrum analyzers implement this type of conversion. One spectrum analyzer is based on a swept-tuned receiver; the other is based on digital signal processing technology. The remainder of this article describes the swept-tuned spectrum analyzer.

Spectrum analyzers are typically used for radio-frequency measurements. Because the measurement bandwidth in the hypersonic-crossflow-transition experiment extended only slightly beyond the audio range, commercially available analog function modules (rather than radio-frequency components) were used in constructing the swept-tuned spectrum analyzer. They included an analog multiplier instead of a mixer, a root-mean-square-to-direct-current (rms-to-dc) converter as an envelope detector, and a digital sine-wave generator combined with a voltage-to-frequency converter for a local oscillator (LO). In lieu of a conventional display, the amplitude and frequency outputs of the analyzer were sampled by a PCM encoder. Then the display was obtained on the ground (where the calibrations were applied) by plotting the amplitude readings against the frequency readings.

The lower part of Figure 2 shows two vibration spectra obtained during one flight. The dashed line represents the vibration level while the rocket was held by the launching aircraft prior to launch; the solid line represents the vibration level at a high angle of attack after ignition of the rocket motor.

Calibration of the spectrum analyzer was done by Philip J. Hamory of **Dryden Flight Research Center**. *Design was done by John K. Diamond of Langley Research Center. Analysis of data was done by Arild Bertelrud of Analytical Services and Materials, Inc. Further information is contained in a TSP* *[see page 1].*

DRC-00-12

System Computes Flow Quantities From Acoustic-Sensor Output

Statistical and neural-network analyses yield information on single- or two-phase flow.

Stennis Space Center, Mississippi

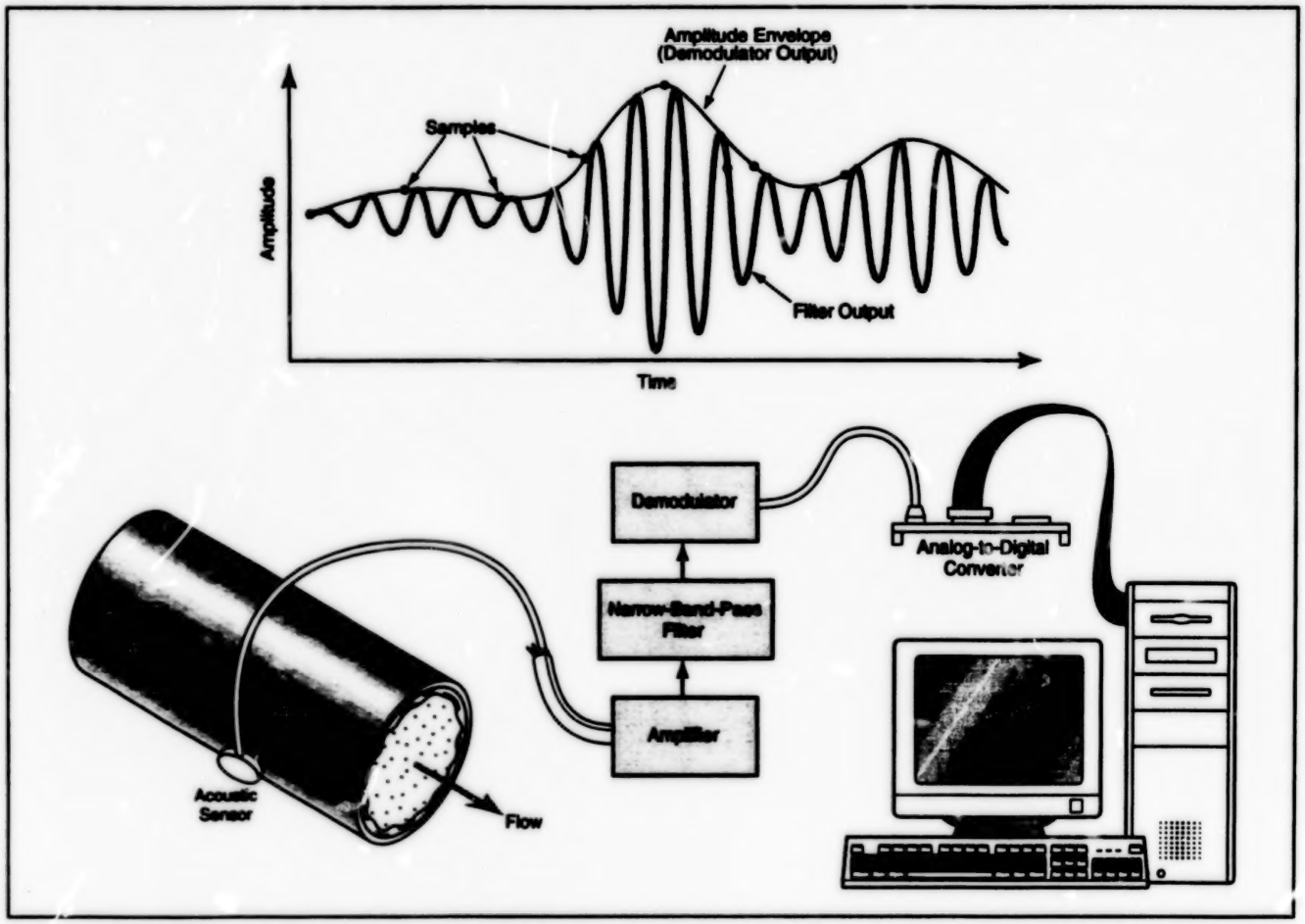

Analog and Digital Electronic Circuits process the output of an acoustic sensor on a pipe. Flow parameters are computed from statistical characteristics of the slowly varying amplitude envelope of the signal in a narrow pass band centered approximately at the resonance frequency of the sensor.

The figure schematically depicts a flow-measurement system based on an acoustic sensor mounted on a pipe, along which flows a single or two-phase fluid. The electrical output of the sensor is processed by an electronic subsystem to estimate various parameters of the flow.

The sensor output is first amplified, then sent through a narrow-band-pass filter with a pass frequency approximately equal to the resonance frequency of the sensor. (A typical acoustic flow sen-

sor has a resonance frequency ≈83 kHz). For the purpose of digital processing to completely characterize the filtered signal, it would ordinarily be necessary to sample and process the signal at a rate of about four times the pass frequency. However, assuming that the sensor resonance is not highly damped, useful data about the acoustic excitation (and thus about the flow that causes the acoustic excitation) can be extracted by measuring the relatively slowly varying amplitude envelope of the filter output.

Accordingly, the output of the filter is demodulated to obtain the amplitude envelope. Because of the relatively slow variation of the amplitude envelope, it is possible to extract sufficient information by digitizing and processing the output of the demodulator at a lower sampling rate (as low as about 33 kHz), which can be implemented much more easily. The digital samples are fed to a computer, which executes special-purpose software to perform a combination of statistical and neural-network processing to obtain flow parameters. The sampling rate is low enough to enable the computer to process the samples in real time.

The statistical flow-indicator quantities calculated by the computer can include the following:

- The average and the standard deviation of the signal amplitude,
- The characteristic autocorrelation time of the variation in the amplitude envelope,
- The average of the absolute value of the difference between successive samples,
- The root mean square of the difference between successive samples,
- The average and the root mean square of the interval between instants when the instantaneous amplitude crosses from below to above the average amplitude, and
- The average and the root mean square of the time between an upward and a downward crossing.

These statistical flow-indicator quantities are fed to a neural network, which calculates the mass flow rate and other flow parameters of interest. A neural network is used for this purpose because of the inherent ability of a neural network to learn nonlinear correlations that involve abrupt transitions, strongly varying behaviors, or complicated interactions among input variables, even in the absence of a mathematical model of the relationships among the input and output variables. As in the cases of other neural networks, this neural network is programmed by training it with numerous sets of examples of inputs (the statistical flow-indicator quantities) and the corresponding outputs (e.g., the mass flow rate in single-phase flow, the presence or absence of a second phase, and separate mass flow rates of liquid and gas in the case of two-phase flow). The analytical methods are described in U.S. patents 5,600,073, 5,717,691, and 5,741,980.

This work was done by Wayne S. Hill and Bruce N. Barck of Foster-Miller, Inc., for **Stennis Space Center.** *Further information is contained in a TSP [see page 1].*

In accordance with Public Law 96-517, the contractor has elected to retain title to this invention. Inquiries concerning rights for its commercial use should be addressed to

Foster-Miller, Inc.
350 Second Ave.
Waltham, MA 02451-1196

Refer to SSC-00053, volume and number of this NASA Tech Briefs *issue, and the page number.*

Improved Eye-Tracking Apparatus

Spurious effects of ambient infrared light have been reduced.

NASA's Jet Propulsion Laboratory, Pasadena, California

A previously developed apparatus that tracks the orientation of the human eye has been modified to make it less susceptible to error induced by ambient infrared light. The apparatus is a commercial product intended primarily for use as a computer-control interface for a person who is physically unable to use a keyboard.

The unmodified apparatus includes a near-infrared source that illuminates the eye, plus an infrared video camera that monitors the eye. The source and camera optics are combined so that the infrared illumination strikes the eye along the optical axis of the video camera. The total video image comprises a bright image of the pupil plus a very bright specular reflection from the cornea. The total video image is processed to obtain a vector between the center of the pupil and the corneal reflection. This vector constitutes the desired information on the orientation of the eye (the gaze direction).

The unmodified apparatus incorporates several features to minimize the effect of ambient infrared light: The infrared source is a narrow-band light-emitting diode (LED) that operates at high power. A band-pass optical filter is placed in front of the video camera to block as much ambient infrared light as possible while passing the infrared light from the LED. Despite these features, infrared light from the Sun, incandescent lamps, and other sources can decrease the signal-to-noise ratio of the pupil and corneal-reflection images so much as to introduce errors or even cause the apparatus to lose track of the eye. Thus, to ensure reliable operation, the unmodified apparatus must be used indoors, with shades drawn to reduce sunlight, and with no incandescent lamps lit (fluorescent lamps are acceptable).

Accordingly, modifications were made to increase the signal-to-noise ratio in the presence of ambient infrared light. The modifications were (1) replacement of the LED by a different LED of narrower spectral width and of greater power within eye-safe limits and (2) replacement of the band-pass optical filter with another one that is better matched to the new infrared LED. The new infrared LED operates at a power of 32 mW in a wavelength band 40 nm wide at a nominal wavelength of 880 nm. The new optical band-pass filter has a wavelength pass band only 10 nm wide. Although the filter wavelength pass band is only 1/4 as wide as the emission wavelength band of the LED, computer simulations nevertheless showed that a greater signal-to-noise ratio could be achieved with this filter than with a filter of 40-nm bandwidth.

The modifications have increased the signal-to-noise ratio by a factor >20. The modified apparatus operates under ordinary indoor lighting, without need to turn off incandescent lamps.

This work was done by John Morookian and James Lambert of Caltech for **NASA's Jet Propulsion Laboratory.** *Further information is contained in a TSP [see page 1].*

NPO-20398

Improved Optical Fallout Monitor

This system can now be calibrated for real-time measurement of fallout in the field.

John F. Kennedy Space Center, Florida

Modifications have been made to upgrade the system described in "Optoelectronic Particle-Fallout Sensor" (KSC-11687), *NASA Tech Briefs*, Vol. 19, No. 4 (April 1995), page 17a. A description of the unmodified version of the system is necessary to place a description of the modifications in context:

This is a portable system that measures fallout of small airborne particles. The system includes a sensor module and a data-acquisition module, both of which are battery-powered and contain microcontrollers and other circuitry. The sensor module can operate either independently or under control by the data-acquisition module.

The sensor module includes a black acetal plastic housing with a top opening through which dust can fall onto a mirror. A portion of the mirror is illuminated by an infrared light-emitting diode (LED). When particles are not present on the mirror (and provided that the mirror is not scratched), the infrared light is reflected specularly by the mirror and absorbed by the black sides and top of the housing. When particles are present, the infrared light that they scatter is measured by a photodetector assembly. The optics are designed to minimize the detection of both ambient light and light scattered from surfaces other than that of the mirror. The photodetector output is amplified, digitized, and time-tagged as an indication of the particulate contamination of the mirror surface as a function of time.

To conserve battery energy, the sensor module is designed to operate for only a few seconds — just long enough to take a reading when it is commanded to do so. When separated from the data-acquisition module, the sensor module is turned on to take a reading by pressing a momentary-contact button switch. To increase sensitivity and facilitate discrimination against background signals, the infrared LED is turned off and on several thousand times during each sampling interval. The difference between the signals measured in the "on" and "off" states is averaged over the sampling interval to produce an output signal that contains relatively low noise.

To operate the two modules together, it is necessary to connect them via a ribbon cable. In this configuration, the data-acquisition module takes control of, and supplies power to, the sensor module. At time intervals selected by the operator, the data-acquisition module commands the sensor module to take readings and records both each reading and the time when it was taken. The module can later be connected to a computer to transfer the reading and time data to the computer for display and/or analysis and to program the data-acquisition module for subsequent readings. This completes the description of the unmodified version of the system.

The modifications were made primarily to overcome the following deficiencies of the unmodified version of the system:

- Sensitivity was not adequate for use in very clean environments;
- It was not possible to calibrate the system accurately by following commonly accepted practices;
- The system was not sufficiently thermally stable for use in non-temperature-controlled environments;
- The electrostatic and power-consumption characteristics did not satisfy requirements for use of the system in certain specific spacecraft-payload-processing clean rooms at Kennedy Space Center;
- It is now a one-piece instrument; and
- The instrument has RS-232 output and can be programmed remotely and used as part of a facility contamination monitor system.

The sensitivity of the system was increased by replacing a 12-bit analog-to-digital converter (ADC) with a new 20-bit ADC. The integrated-circuit chip of which the 20-bit ADC is a part affords additional digital filtering capabilities, which are exploited to increase the robustness of operation under adverse lighting situations. To accommodate the aforementioned circuitry, a circuit board was completely redesigned, with special attention paid to quality of signal and reliability. The redesigned circuit board supports additional features, including programming of operating parameters via a keypad, a current-loop or voltage analog output, and new power-utilization features. The overall number of integrated-circuit chips has been reduced, and the number of circuit boards has been reduced from 2 to 1.

The system now operates on modified software that provides, among other things, the ability to reprogram "on the fly" (without disrupting operation) to adjust such parameters as sensitivity ranges and data-taking intervals. (Previously, it was necessary to turn the system off, then back on again to put it in a programming mode.) The modified software makes it possible to reprogram or to download data from the system remotely by serial data communication via a cable.

A reference photodetector with an independent ADC was added. These components will make it possible to measure and hence correct for fluctuations in the output of the LED, thereby increasing the temperature stability of the system by an order of magnitude.

The mirror in the unmodified version of the system was replaced with a witness plate in the form of a silicon wafer bonded to an aluminum substrate. Holes in the aluminum substrate make it possible to scan the silicon wafer, by use of a semiconductor-wafer scanner, for extremely accurate analysis of the particulate contamination on the wafer; this makes it possible to perform acceptable calibration.

The optics have been simplified to reduce the number of surfaces through which light must pass, thereby increasing throughput of the light to the photodetectors. There is also now an option to use an LED with a wavelength of 935 nm in applications in which the shorter wavelength (880 nm) of the unmodified system would be problematic.

The electronic circuitry was modified to enable the system to operate on intrinsically safe power through an intrinsically safe barrier to enable use in hazardous environments. Finally, the electrostatic-charge issue was addressed by repackaging the system in an aluminum enclosure, which can be grounded.

This work was done by Paul A. Mogan of **Kennedy Space Center** *and Christian J. Schwindt, Timothy R. Hodge, and Steven J. Klinko of Dynacs Engineering Co. Inc. Further information is contained in a TSP [see page 1].*

This invention has been patented by NASA (U.S. Patent No. 5,412,221). Inquiries concerning nonexclusive or exclusive license for its commercial development should be addressed to the Technology Programs and Commercialization Office, Kennedy Space Center, (407) 867-6373. Refer to KSC-12105.

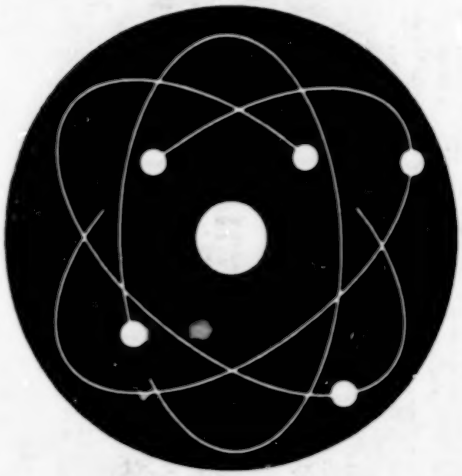

Physical Sciences

Hardware, Techniques, and Processes

19 Array of Microscale Heaters and Heat-Flux Sensors
20 Inexpensive, Rugged Oxygen Sensors Qualified for Flight
21 High-Temperature, Fiber-Optic-Readout Pressure Transducers
22 Miniature Birefringence-Measuring System
23 Parallel-Beam Interferometry With Incoherent Light
24 Correcting for Atmospheric Effects in Optical Communication
25 Detecting Hydrazine via Optical Detection of Ammonia

Books and Reports

25 Dislocation-Induced Changes in $In_xGa_{1-x}As$ Quantum Dots
26 Spaceborne Telescope for Communication, Ranging, and Imaging
26 Solitons on WDM Beams in a Nonlinear Optical Fiber

18

BLANK PAGE

Array of Microscale Heaters and Heat-Flux Sensors

Heat transfer in boiling can be measured with unprecedented spatial and temporal resolution.

John H. Glenn Research Center, Cleveland, Ohio

A device has been developed for measuring heat-transfer rates at many points underneath individual bubbles during boiling, in order to determine the heat-transfer coefficient as a function of position and time. The device is a planar array of small heaters that also serve as heat-flux sensors.

Heretofore, the majority of experimental data on heat transfer in boiling have been obtained by use of devices as large as or larger than bubbles; consequently, the data have not been spatially resolved to dimensions smaller than those of bubbles, and little has been learned about local heat-transfer rates from wall surfaces under and around the bubbles as the bubbles grow and depart from the walls. The present device enables measurement of the local heat transfer from a wall surface during the growth and departure of a bubble, with very high temporal and spatial resolution. Thus, the present device is expected to contribute to better understanding of boiling heat-transfer mechanisms by indicating when and where in the bubble-departure cycle large amounts of heat are transferred from the wall. The information provided by this device could be used to validate or improve analytical and numerical models used in computational simulations of boiling. Other uses for temporally and spatially resolved heat-transfer data obtained by use of this device and similar devices include identification of time-varying structures in near-wall regions of turbulent boundary layers or impinging jets, study of heat-transfer coefficients associated with spray cooling processes, and determining shear stresses in turbulent flows.

The device (see figure) includes a quartz substrate that supports a square array of 96 electrical-resistance heaters. Each heater occupies an area of 250 by 250 μm. The resistive heating element in each heater is a platinum strip 5 μm wide, 0.4 μm thick, and 6 mm in total length; the lateral gap between adjacent parallel portions of the strip is 5 μm. Each strip has an electrical resistance of ≈1 kΩ with a temperature coefficient of resistance of 2×10^{-3} °C^{-1}. Heater power is supplied through aluminum lines routed between the heaters to the edge of the array.

Each heater strip is electrically connected to one of the resistances in a Wheatstone bridge. The resistance (and thus the temperature) of the bridge is kept at a constant desired value by use of a feedback control circuit similar to circuits used in hot-wire anemometry. The circuit constantly adjusts the power supplied to the heater to keep the Wheatstone bridge balanced. Thus, the instantaneous power supplied to the heater is a measure of the local heat-transfer coefficient in that it equals the rate at which heat must be supplied to keep the affected portion of the surface at the desired temperature (e.g., the temperature of the wall in contact with the boiling liquid).

Because the heater strip is so thin, the frequency response of the heater greatly exceeds typical frequencies associated with boiling, making it possible to measure heat-transfer coefficients with high temporal resolution. The spatial resolution is, of course, determined by the pitch of the array.

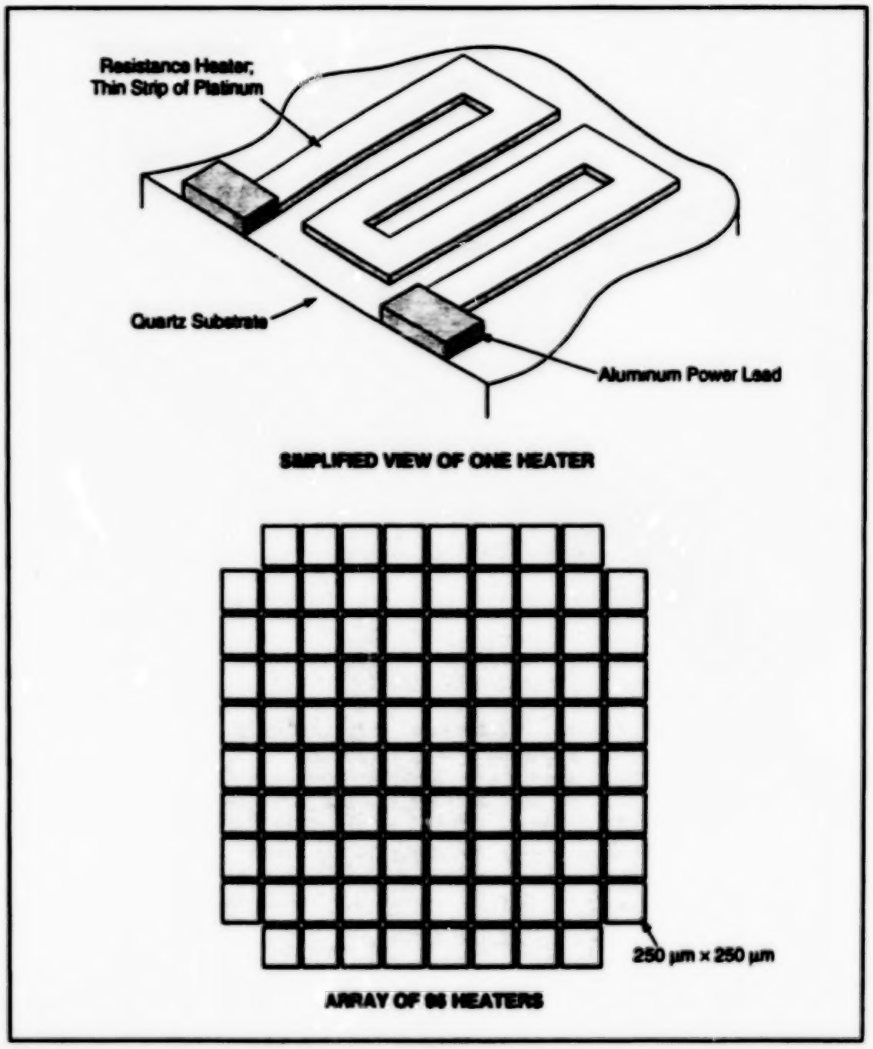
Resistance Heater; Thin Strip of Platinum
Quartz Substrate
Aluminum Power Lead
SIMPLIFIED VIEW OF ONE HEATER
250 μm × 250 μm
ARRAY OF 96 HEATERS

Ninety-Six Thin-Film Electrical-Resistance Heaters in a square array are kept at constant electrical resistance and thus constant temperature. The instantaneous power supplied to each heater is a measure of the instantaneous local heat-transfer coefficient.

This work was done by Jungho Kim formerly of the University of Denver and Richard Quine of the University of Denver for **Glenn Research Center**. *Further information is contained in a TSP [see page 1].*

Inquiries concerning rights for the commercial use of this invention should be addressed to NASA Glenn Research Center, Commercial Technology Office, Attn: Steve Fedor, Mail Stop 4–8, 21000 Brookpark Road, Cleveland, Ohio 44135. Refer to LEW-16825.

Inexpensive, Rugged Oxygen Sensors Qualified for Flight

These sensors satisfy requirements for safety in flight tests.

Dryden Flight Research Center, Edwards, California

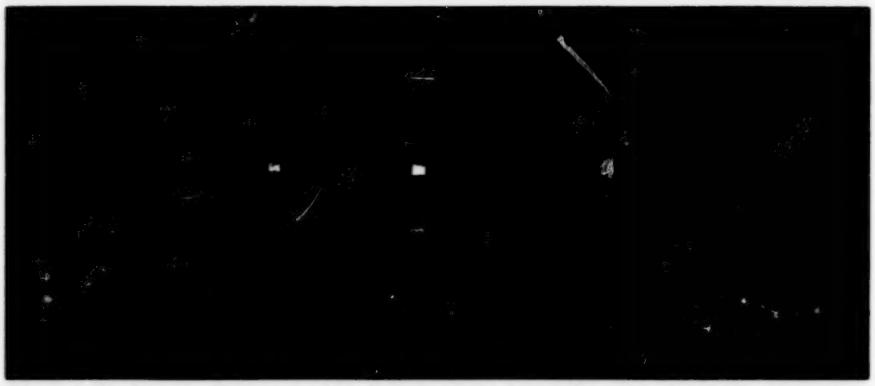

Figure 1. An Oxygen Sensor and Its Temperature Controller were electrically connected and packaged separately.

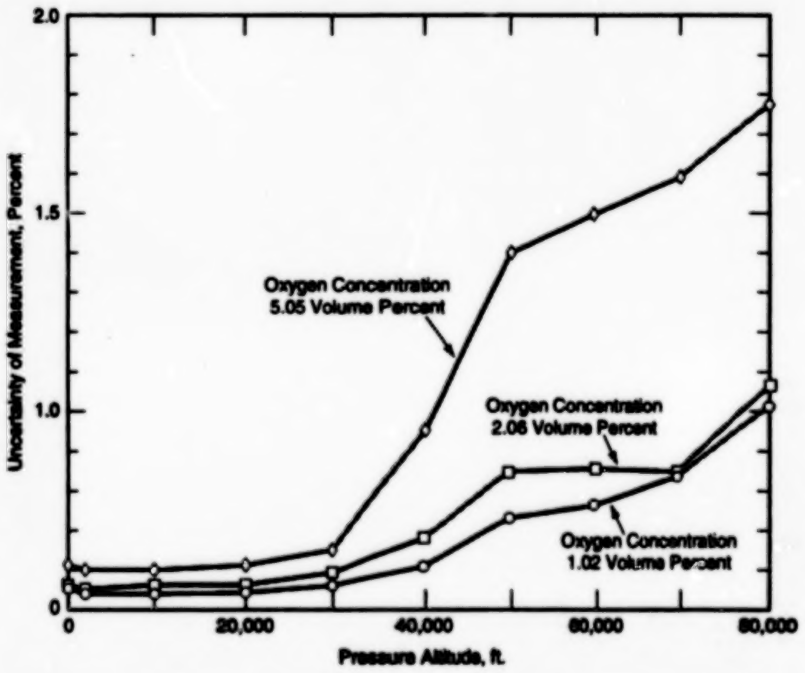

Figure 2. The Uncertainty of Measurement as a function of pressure altitude was computed for various concentrations of oxygen for a 99-percent confidence level after correction.

NASA Dryden Flight Research Center has ruggedized and qualified an inexpensive commercial off-the-shelf (COTS) oxygen sensor that accurately and reliably aids assessment, in flight tests, of the hazards associated with propulsion systems supplemented by oxidizers. Future flight-test vehicles continue to rely on such energetic propellants as liquid and/or gaseous oxygen and hydrogen for purposes of demonstration because these propellants deliver high specific impulses.

In preparation for flight testing in the Linear Aerospike SR-71 Experiment (LASRE) program, commercial sensors intended originally for medical and automotive application were qualified for flight. After a rigorous process of qualification and calibration, the sensors proved extremely reliable and repeatable, and gave engineers the confidence they needed to assess the hazard of flammability during test operations. These sensors have now been added to the Hyper-X program and are scheduled for use in future flight-test projects. (The Hyper-X is a proposed experimental hydrogen-fueled hypersonic aircraft.)

The sensor in question is a commercial-grade miniature fuel cell — in other words, a small transducer that converts chemical energy into electrical energy. Like all electrochemical transducers, a sensor of this type contains an anode, a cathode, and an electrolyte. At the cathode, during operation, oxygen molecules are reduced to hydroxyl ions. The anode is made of lead; during operation, lead in the anode becomes oxidized to lead oxide, producing two electrons for each atom of lead thus consumed. This particular transducer has cross-sensitivity only to other gases (e.g., halogens) that oxidize leads.

The sensor life expectancy has been estimated by the vendor to be approximately 2.4 years. However, because of the criticality of these sensors, it was decided that in the LASRE project, each such sensor will be replaced when its response deteriorates or it reaches a calendar life of 1.5 years.

In the laboratory calibration tests, the sensor was actively maintained at a temperature ≈115 °F (≈46 °C) to prevent freezing of the electrolyte (which is aqueous) as well as to maintain constant performance of the transducers throughout the flight envelope. Each sensor was inserted into an aluminum tube shell for structural support. Attached to the shell was a thin-film resistive heating element, a power transistor, and two resistance temperature devices (RTDs). In addition, thermal-insulation material was wrapped around the shell. The power to the heating element was regulated by a heater-controller circuit in a box separate from the sensor (see Figure 1), in response to temperature feedback from the first RTD. The second RTD was used for monitoring and to provide a temperature reading as part of the sensor output.

At the initial application of power, the heating element was activated until the transducer assembly reached the set temperature. Once the set temperature was reached, the power to the heating element was cycled on the basis of the reading of the first RTD. During application of power to the heating element, the heater controller draws an electrical current <1/2 A.

In initial flight tests, it was found that two-point calibrations were not satisfactory for the use of these instruments in flight tests. A calibration test was designed to enable the attainment of the following three test objectives: (1) characterize sensor behavior with increasing altitude (decreasing partial pressure), (2) perform a statistical analysis

of laboratory-test results (which analysis would give a quantitative measure of the level of confidence in the mean of the untested sensors), and (3) quantify the uncertainty of the sensor measurements with decreasing partial pressure. Several of the sensors were installed in a small test chamber and exposed to the following range of O_2 concentrations (volume percentages) with nitrogen balances: 0, 1.02, 2.06, 5.05, 10, and 21. Each sensor was cycled through a range of pressure altitude from sea level up to 80 kft (24 km) and then back down to sea level. During this cycle, the sensor output was measured at intervals of 10 kft (3 km), using the concentrations listed above.

Because of a nonlinear response that occurred during operation above 30 kft (9 km), an altitude correction factor was devised. This correction factor was computed in the following procedure: The ratio between (1) the true partial pressure of oxygen (as determined by use of the calibration gases) and (2) the transducer output was determined for each altitude. This ratio was then plotted against altitude, and the data of this plot were fitted with a fifth-order curve. During the flights, the correction factor was computed from the fifth-order curve. This correction factor was then multiplied with the linearly calibrated transducer output to produce an altitude-corrected partial-pressure reading. Normalization of this value by the static-pressure measurement yielded an output volume fraction. On the basis of the *t* distribution of the corrected readings, the uncertainty was found to remain less than one percent for altitudes less than 60 kft (18 km), as shown in Figure 2.

Twelve of the sensors and their respective thermal controllers were integrated into the LASRE flight-test fixture and were flight-tested out to a speed of mach 1.6 and an altitude of 52 kft (16 km). Eight of the original twelve sensors remained on board after removal of the LASRE for some follow-on flight tests at speeds up to mach 3.03, altitudes to 73 kft (22 km), and exposure to internal temperatures >130 °F (>54 °C). Even though the temperatures rose above the temperature-controller limits and the manufacturer's specifications for operation, the oxygen sensors exhibited no significant drift.

Four sensor suites are to be incorporated into the Hyper-X airplane for safety during the flight test in which the Hyper-X will be carried by a B-52 airplane. These sensors will be used to verify the desired and expected chemical inertness (more specifically, the lack of oxidizing gas) in the interior of the vehicle. They are being calibrated in much the same manner as in the LASRE program, but dynamic-response and sensor-recovery tests will be performed in addition, for comparison with results of tests in the boost and free phases of the flight of the Hyper-X.

This work was done by Neal Hass, Michele Jarvis, and Kim Ennix of **Dryden Flight Research Center.**
DRC-00-04

High-Temperature, Fiber-Optic-Readout Pressure Transducers

These transducers could be mounted in harsh environments like those inside turbine engines.

John H. Glenn Research Center, Cleveland, Ohio

Fiber-optic-coupled differential-pressure transducers are being developed for use in hot, harsh environments like those in the cores of aircraft turbine engines. The prior approach to the measurement of pressures in such engines involves the use of pressure transducers coupled to pressure taps via long tubes, which introduce delays and degrade responses to high-frequency pressure variations. In contrast, the fully developed versions of the developmental transducers would be mounted directly in the affected compressor, combustor, and turbine stages; because there would be no long pressure-coupling tubes, these pressure transducers would yield more-accurate readings in more nearly real time. The readings could help to identify conditions that must be corrected in maintenance work and could, potentially, enhance safety in flight by providing indications of impending compressor stall.

The developmental fiber-optic-coupled differential pressure transducers are denoted twin-column transducers (TCTs) for a reason that will immediately become apparent: A transducer of this type includes two tubes (T1 and T2), nominally of identical length and width. The tubes are sealed at their tips and are connected at their bases to sources of the differential pressure to be measured (see figure). Upon pressurization, each tube becomes slightly elongated — by an amount proportional to the difference between its interior pressure and the ambient pressure. Similarly, if a tube is partly or wholly evacuated, it is proportionately shortened. Thus, the differential elongation of the two tubes is proportional to the differential pressure between their interiors. The twin-column design automatically compensates for temperature; that is, any change in ambient temperature affects both tubes nearly equally and thus does not appreciably alter the differential elongation.

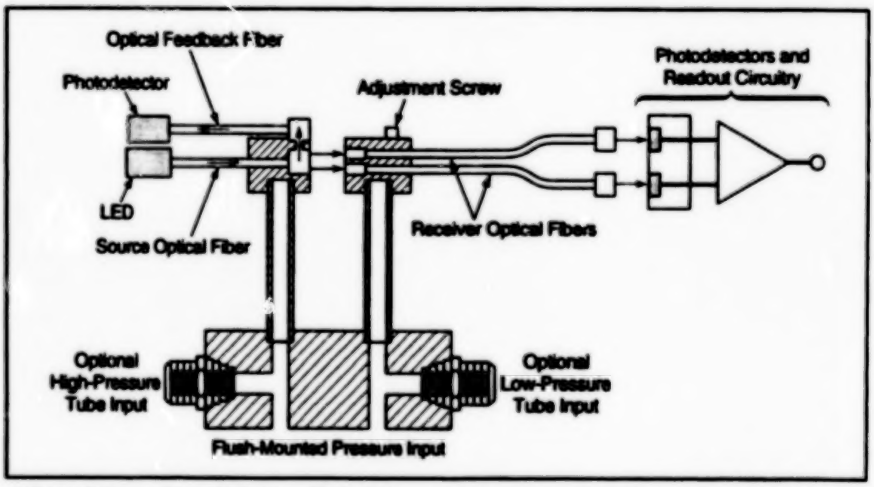

A Twin-Column Transducer is a differential-pressure transducer that inherently has a high degree of temperature compensation. Differential pressure in the tubes is determined from fiber-optic measurement of differential elongation of the tubes.

The tips of the tubes are capped with assemblies for input and output coupling of light via optical fibers, which are arranged for measuring the differential elongation of the tubes. Input light from a light-emitting diode (LED), provided via a source optical fiber, is aimed from the assembly on T1, across the gap to two receiver optical fibers in the assembly on T2. The positions of the fibers are adjusted so that (1) when the differential elongation of both tubes is zero

(corresponding to zero differential pressure), equal amounts of light are coupled into both receiver fibers; (2) any nonzero differential elongation of the tubes gives rise to a proportional imbalance between the amounts of light coupled into the receiver fibers; and (3) the sum of amounts of light coupled into both receiver fibers remains constant as the differential elongation changes. As a result, the ratio between the difference and the sum of the receiver-fiber outputs is proportional to the differential pressure.

The LED and the photodetectors and electronic circuitry used to process the output light from the receiver fibers are located safely away from the hostile environment of the TCT. An additional optical fiber can be installed on the T1 side to provide feedback for regulating the intensity of light emitted by the LED; such feedback regulation renders the final differential-pressure reading relatively insensitive to fluctuations of temperature and voltage in the electronic circuitry.

The key components that are expected to make high-temperature TCTs possible are low-loss optical fibers capable of transmitting light between hot engine locations and cooler remote locations where electronic circuitry can be operated in safety. Sapphire optical fibers several meters long, with losses of less than 0.2 dB/km have been fabricated experimentally. A practical design might provide for short lengths of high-quality sapphire fibers from the point of measurement, coupled to less-expensive commercial sapphire fibers of lower optical quality, and finally to low-loss, low-temperature optical fibers to cost-effectively bring signals out through zones of progressively decreasing ambient temperature.

This work was done by Charles A. Liucci of LEL Corp. for **Glenn Research Center.**

Inquiries concerning rights for the commercial use of this invention should be addressed to NASA Glenn Research Center, Commercial Technology Office, Attn: Steve Fedor, Mail Stop 4–8, 21000 Brookpark Road, Cleveland, Ohio 44135. Refer to LEW-16889.

Miniature Birefringence-Measuring System

Advantages over older systems include compactness, light weight, low power consumption, and greater sensitivity.

John H. Glenn Research Center, Cleveland, Ohio

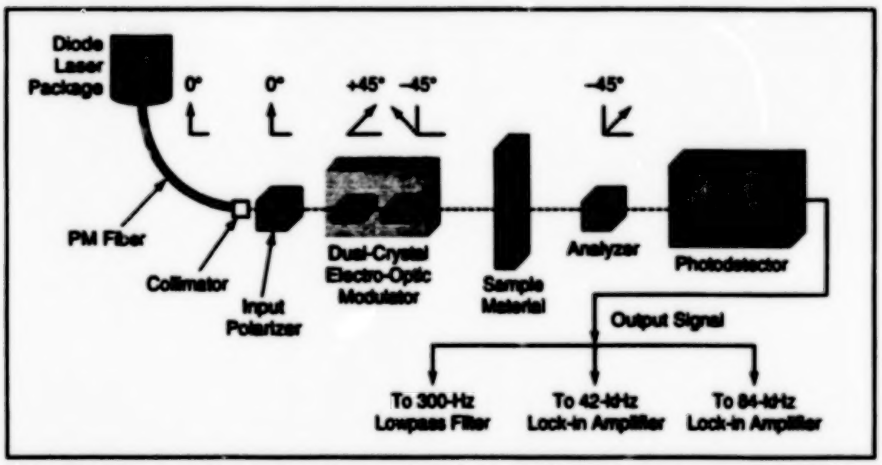

This Birefringence-Measuring System includes a dual-crystal electro-optical modulator, which is depicted here schematically in its geometric relation to polarization and to the other optical components.

A miniature birefringence-measuring system has been developed for use in investigating extensional flows of non-Newtonian polymers in microgravity. The system could also be used on Earth to perform general optical-retardation and dichroism measurements, to measure stresses with high sensitivity, to characterize polymers, and to measure orientation angles of molecular chains. The system includes a dual-crystal transverse electro-optical phase modulator that makes it possible to measure small (of the order of 10^{-9}) changes in the birefringence of a material under test as the material is subjected to extensional deformation or shear stress. Moreover, because the modulation frequency can be > 100 MHz, it may be possible to use the system to study chaotic flow birefringence.

Previously developed phase-modulation birefringence-measuring systems have traditionally been built around single-crystal photoelastic modulators (PEMs). One representative fused-silica PEM assembly for visible light weighs 9.1 kg and has a 27-mm useful aperture. A typical previously developed system can occupy 2 m of lineal space. Given these typical weight and size parameters, previously developed systems are too heavy and large for many applications. In contrast, the present miniature birefringence-measuring system weighs only about 2.5 kg and occupies only 28 cm of lineal space. In addition to smaller size and weight, the advantages of this system over previously developed birefringence-measuring systems include lower power consumption, greater robustness, shorter warmup time, and greater accuracy and sensitivity in the birefringence measurement.

The modulator in this system is a commercially available one that contains two $LiNbO_3$ crystals oriented with their principal axes orthogonal to each other and at ±45° with respect to the polarization of incident laser light. The figure depicts the basic optical configuration. The second crystal is needed to counteract effects of thermal instability because the static birefringence of $LiNbO_3$ is highly temperature-dependent. In addition, when the modulation voltage applied to the second crystal is 180° out of phase with that applied to the first crystal, the effective modulation depth is doubled.

The system has been calibrated by incrementing the modulator driver voltage and mapping the appropriate Bessel functions. Calibration data were taken at 500 points, and the experimentally generated calibration curves were found to agree with the expected curves at every data point with a worst correlation error of less than 0.5 percent. This is an order of magnitude better than the accepted calibration standard, for which the worst correlation error ranges from 2 to 5 percent. This system has also been tested against a PEM-based birefringence-measuring system, with favorable results.

This work was done by Jeffrey R. Mackey of Analex Corp. for **Glenn Research Center.** *Further information is contained in a TSP [see page 1].*

Inquiries concerning rights for the commercial use of this invention should be addressed to NASA Glenn Research Center, Commercial Technology Office, Attn: Steve Fedor, Mail Stop 4–8, 21000 Brookpark Road, Cleveland, Ohio 44135. Refer to LEW-16705.

Parallel-Beam Interferometry With Incoherent Light

It should be possible to achieve resolution beyond the diffraction limit.

NASA's Jet Propulsion Laboratory, Pasadena, California

A technique of parallel-beam interferometry with spatially incoherent light has been proposed to solve two problems that arise in conjunction with using interferometry to measure the shape of a surface. The first problem is how to obtain spatial resolution in excess of the diffraction limit; the second problem is how to measure the variation in the shape of an object with temperature.

Figure 1 illustrates the principle of operation. Spatially incoherent light (e.g., light from an incandescent lamp) would be collimated, then made to pass through beam-splitting-and-combining optics that would split the light into two parallel beams aimed toward the object of interest. These optics would be adjustable to change the distance between the two beams. The light reflected by the object would pass back through the beam-splitting-and-combining optics which combine the two beams back into a single beam, then through imaging optics into a camera. Objective optics may or may not be used, as explained below.

The technique can be characterized as one that utilizes speckle interferometry with a variable speckle. The splitting of the source incoherent beam into two parallel beams introduces a delta-function spatial coherence that gives rise to a speckle interference in the camera. The speckle pattern is measured as the distance between the two beams is changed. The change in distance changes the location of the delta function in the spatial coherence, and a spatial autocorrelation function is measured. The surface of the object of interest can be determined accurately from the autocorrelation function. Under ideal conditions, resolution beyond the diffraction limit can be achieved.

The solution to the second problem would have to involve utilization of the speckle interferometry in ways that would make it unnecessary to scan the beams. One such way would be to form more than one interference pattern by use of more than two beams, in a generalization of the basic concept that involves several two-beam interferometers working together.

Figure 2 presents an example of a parallel-beam interferometer according to the proposal. A collimated beam of light would pass through an assembly of beam splitters and prisms. The first beam splitter together with the second beam splitter would cause both beams to traverse the same path (and thus the same path length) in opposite directions; this would ensure that white-light fringes would be imaged on the camera. The objective optics may or may not be used, depending on the required numerical aperture, which, in turn, would determine the diffraction-limited imaging resolution. The two beam splitters and the right-angle prism would be moved together to change the distance between the two beams without changing the difference between their optical-path lengths.

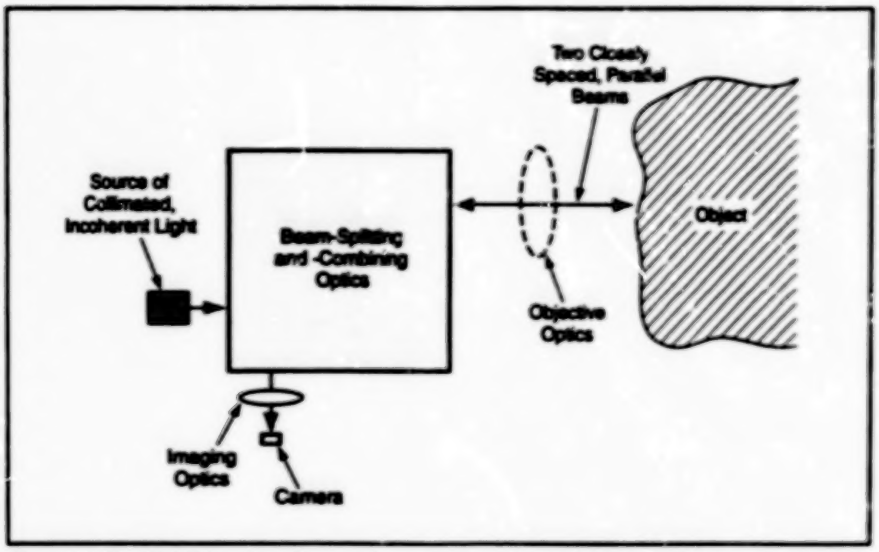

Figure 1. In Parallel-Beam Interferometry, an object would be illuminated with two closely spaced, parallel beams generated by splitting a single input beam. The distance between the parallel beams would be adjustable in any direction in the plane perpendicular to the axis of propagation.

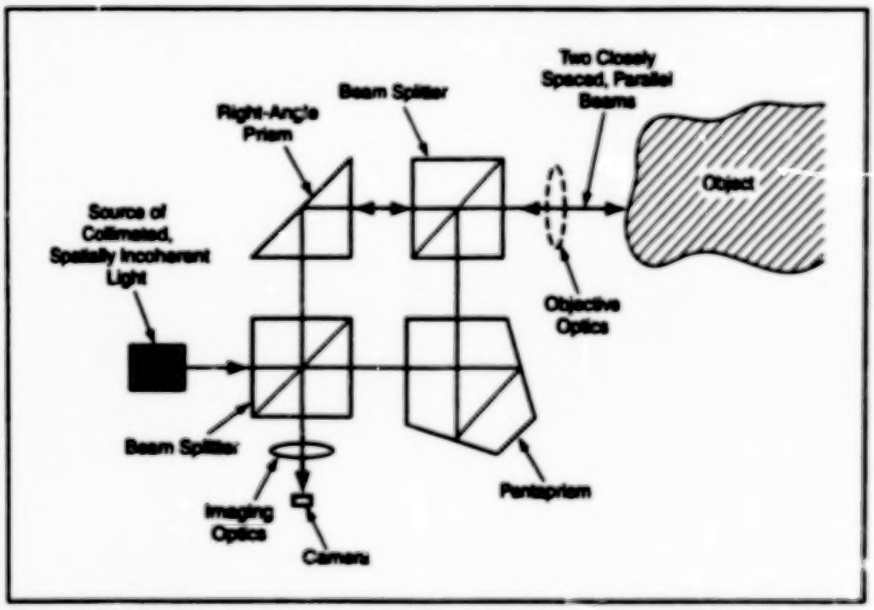

Figure 2. This Optical Layout is one of several candidate layouts for a practical parallel-beam interferometer. The two nonpolarizing beam splitters and the prism would be moved in coordination to adjust the distance between the parallel beams.

In addition to resolution beyond the diffraction limit, the proposed technique would afford several other advantages over prior interferometric imaging techniques:

1. The distance to the object could be set arbitrarily.
2. The alignment of the object with the interferometer would be simplified.
3. Because the two beams would be of the same magnitude, regardless of the reflectivity of the object, the visibility of

the fringes would be relatively high.

4. Because the two beams would travel along nearly the same path, effects of variations in the index of refraction of air would be relatively small. Only high-frequency index variations like those associated with turbulence would be problematic.
5. Imaging could be done with very small numerical apertures, so that it would be possible to use working distance longer and optics smaller than those customarily used.

This work was done by Roman C. Gutierrez of Caltech for NASA's Jet Propulsion Laboratory. Further information is contained in a TSP [see page 1].

In accordance with Public Law 96-517, the contractor has elected to retain title to this invention. Inquiries concerning rights for its commercial use should be addressed to

Technology Reporting Office
JPL
Mail Stop 122-116
4800 Oak Grove Drive
Pasadena, CA 91109
(818) 354-2240

Refer to NPO-20087, volume and number of this NASA Tech Briefs issue, and the page number.

Correcting for Atmospheric Effects in Optical Communication

Distortions of a downward-propagating beam would be used to correct an upward-propagating beam.

NASA's Jet Propulsion Laboratory, Pasadena, California

A method of correcting for the distorting effects of the atmosphere upon a laser beam used in free-space optical communication has been proposed. The original version of the method would be applied to a system in which a laser beam would be transmitted from a ground station to a precisely flat and precisely oriented mirror on a spacecraft in orbit around the Earth, then relayed to a distant spacecraft by reflection from the mirror (see figure). Because propagation of the beam in outer space would be distortionless, the method addresses only the distortions that would arise along the ground-station/near-Earth-spacecraft path.

In the original application, in order to send a sufficiently strong signal to the distant spacecraft, it would be necessary to deliver an approximately diffraction-limited, undistorted laser beam to the orbiting mirror for relay to the distant spacecraft. Therefore, at the ground station, adaptive optics would be used to apply compensatory predistortions to cancel the optical distortions (tilt and scintillation) introduced by the atmosphere. The control signals for the adaptive optics would be generated as explained next.

A small laser aboard the near-Earth spacecraft would transmit a reference beam to the ground station. Because it would propagate along the same path as that of the main communication beam, the reference beam would undergo essentially the same distortions. Thus, measurement of the tilt and scintillation of the reference beam arriving at the ground station would provide the information needed to control the adaptive optics to apply the compensatory predistortions.

To compensate for the predictable aberration caused by orbital motion of the relay mirror, the reference laser would have to be offset from the relay mirror by an angle (as seen from the ground station) of $2v/c$ radians in the plane of relative motion, where v is the component of orbital velocity orthogonal to the optical path and c is the speed of light. For a typical orbit, the offset distance for this angle would be no more than about 8 m.

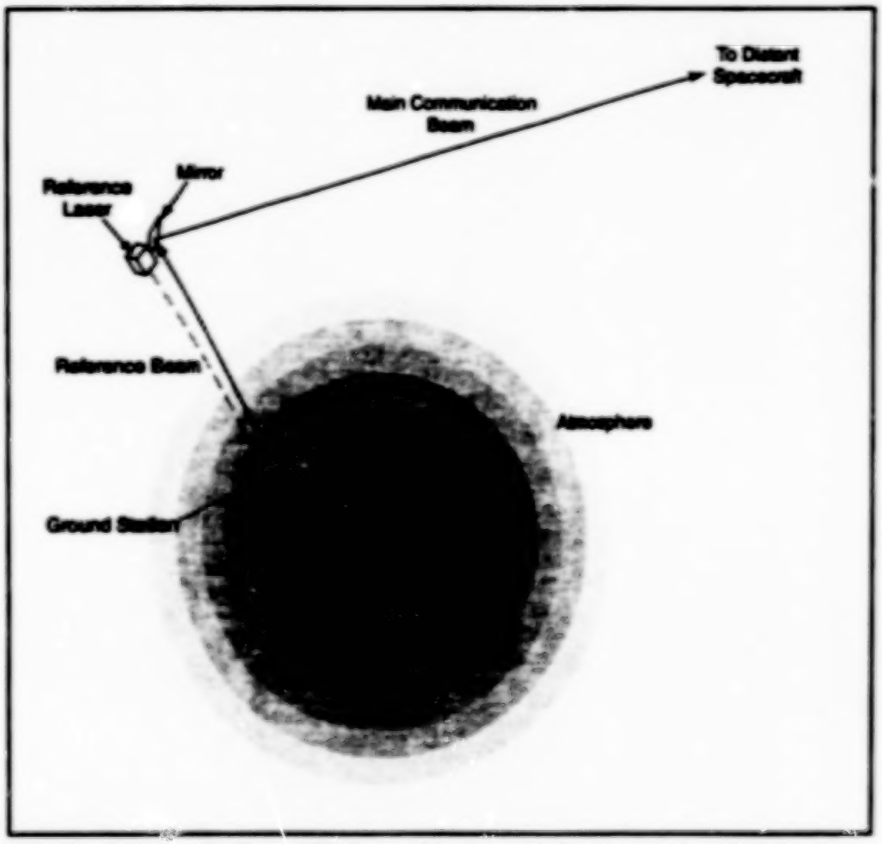

Adaptive Optics at the Ground Station would compensate for atmospheric optical distortions. The information for controlling the adaptive optics would be obtained from measurements of the reference beam.

The reference beam arriving at the ground station must be bright enough that measurements and corrections can be completed within an interval of about 1 millisecond, which is dictated by the temporal variation of atmospheric optical distortion. This requirement turns out not to be especially severe: for example, it has been estimated that even during the day, the beam from a reference laser with a wavelength of 0.5 μm, a power of 1 mW, and optics with an aperture diameter of about 10 cm, located in a geosynchronous orbit, would be sufficiently bright for measurement through a ground telescope with an aperture diameter of about 1 m and a band-pass optical filter.

This work was done by John Armstrong, Cavour Yeh, and Keith Wilson of Caltech for NASA's Jet Propulsion Laboratory. Further information is contained in a TSP [see page 1].

NPO-20506

Detecting Hydrazine via Optical Detection of Ammonia

An ammonia signal would be indicative of hydrazine because hydrazine decomposes to ammonia.

NASA's Jet Propulsion Laboratory, Pasadena, California

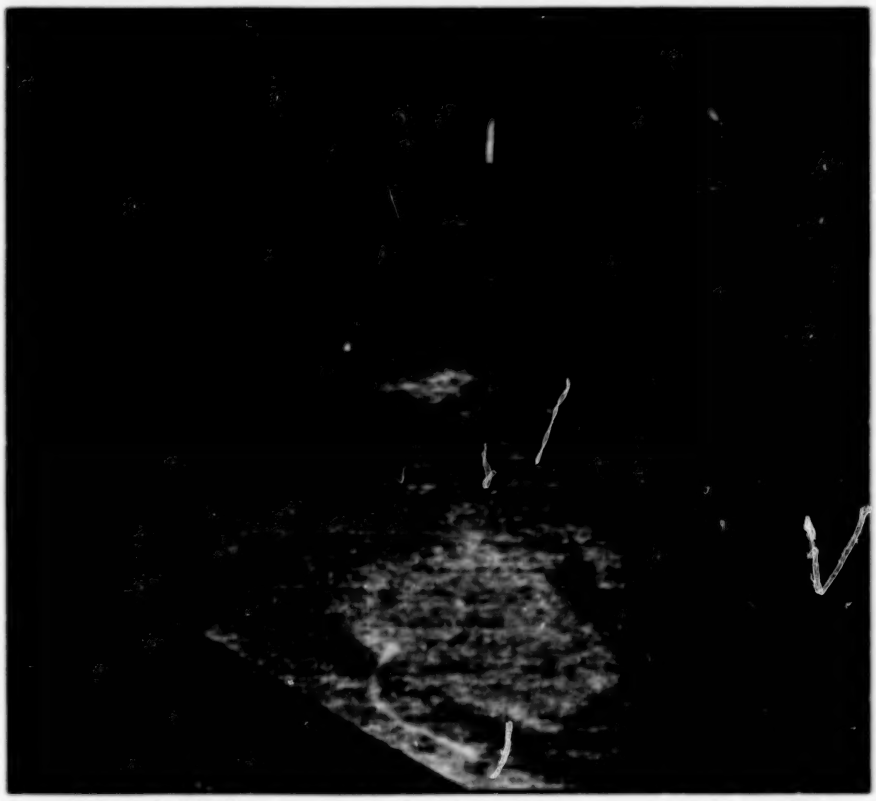

Laser Beams of a TDL Spectrometer are reflected several times across a sample space. The proposed instrument could have a similar optical configuration and would utilize two laser beams: one for detecting hydrazine and one for detecting ammonia.

In a proposed method for rapidly detecting hydrazine in air at concentrations at or above 10 parts per billion by volume (ppbv), tunable diode lasers (TDLs) and photodetectors would be used to measure infrared absorption spectra of both ammonia and hydrazine simultaneously. In this method, one would take advantage of the fact that (1) ammonia is formed in the decomposition of hydrazine and is always present when hydrazine is present and (2) the spectral features attributable to ammonia are much stronger than those attributable to hydrazine, and thus ammonia can be detected more easily. In a typical situation in which hydrazine is suspected of leaking and in which one could rule out an alternative source of ammonia (e.g., an open bottle of household ammonia solution or window cleaner), an ammonia spectrum could thus be taken as an indication of hydrazine.

This method could be implemented by a variety of TDL spectrometers. A typical instrument would include a sample cell, one end of which would be occupied by a sensor head containing two near-infrared TDL/photodetector pairs (one pair for hydrazine and one for ammonia) capable of operating at room temperature. A mirror or a retroreflector would also be included on the sensor head. A retroreflector would be mounted on the other end of the sample cell. The various optical components would be positioned and oriented to make each laser beam traverse the cell multiple times to obtain a total optical path length of 40 m. The instrument might resemble the one shown in the figure, which is a previously developed TDL spectrometer. On the basis of previous experience with TDL spectrometers, the proposed instrument could be expected to weigh 5 to 10 lb (≈2.3 to 4.5 kg).

The atmosphere to be sampled would be drawn through the sample cell, the interior of which would be maintained at a pressure of 0.1 atm (≈10 kPa). Extrapolation from experiments on similar instruments indicates that the proposed instrument could detect hydrazine in a concentration as low as 20 ppbv and ammonia in a concentration as low as 2 ppbv. Thus, although the instrument could not measure hydrazine concentrations below 20 ppbv, it could nevertheless give a warning that hydrazine is likely to be present.

This work was done by John Houseman, Chris Webster, Randy May, and Mark Anderson of Caltech for NASA's Jet Propulsion Laboratory. Further information is contained in a TSP [see page 1].
NPO-20680

Books and Reports

Dislocation-Induced Changes in $In_xGa_{1-x}As$ Quantum Dots

A report describes an experimental investigation that revealed a previously unknown type of spatial alignment of quantum dots (QDs) in $In_xGa_{1-x}As/GaAs$ multilayer structures. Multilayer arrays of QDs (in the form of nanometer-sized $In_xGa_{1-x}As$ islands) were formed by alternately depositing 10-nm-thick layers of GaAs and 5-molecule-thick layers of $In_{0.5}Ga_{0.5}As/GaAs$ on substrates of semi-insulating [001] GaAs with a 2° miscut toward the [101] direction (resulting in steps along the [010] direction). Specimens were examined by electron microscopy and cathodoluminescence (CL) spectroscopy. The QDs were observed to undergo a transition between step edge alignment along the [010] direction to counter step alignment (along the [100] direction). This transition apparently occurred when (or soon after) the fifth quantum-dot layer was deposited, and is apparently associated with the onset of a network of misfit dislocations at the $In_{0.5}Ga_{0.5}As/GaAs$ interface. A change to larger QDs in smaller concentrations was also observed after formation of the network of dislocations. Strong near-infrared CL emission from the QDs was observed, despite the presence of dislocations.

This work was done by Rosa Leon of Caltech for **NASA's Jet Propulsion Laboratory**. *To obtain a copy of the report, "Dislocation-induced changes in quantum dots: step alignment and radiative emission," see TSP's [page 1].*
NPO-20695

Spaceborne Telescope for Communication, Ranging, and Imaging

A report describes a program to develop a multi-function telescope to be carried aboard spacecraft of the planned X2000 series of planetary missions. [A related multi-function telescope was described in "Telescope for Imaging and Laser Communication" (NPO-20388), *NASA Tech Briefs*, Vol. 24, No. 1 (January, 2000), page 27a.] An important element of this program is minimization of instrument mass through combination of several optoelectronic subsystems into one telescope system with one aperture for transmission and reception of light. The functions to be performed by the telescope system include scientific imaging, reception of laser-altimeter return signals, and two-way optical communication. The communication functions include transmission of scientific data, reception of commands, and reception and retransmission of laser ranging signals. For communication, the telescope would be aimed at the sunlit Earth, by use of aiming techniques like those summarized in the cited previous article. Rates for transmission of scientific data to Earth from as far away as Jupiter would range from 100 kb/s (day) to 400 kb/s (night). The data rate for reception of commands from Earth would be 2 kb/s. A flight-qualified engineering model of the system is scheduled for completion in the year 2001.

This work was done by James Lesh and Hamid Hemmati of Caltech for **NASA's Jet Propulsion Laboratory**. *To obtain a copy of the report, "Laser Communications Terminal for the X2000 Series of Planetary Missions," see TSP's [page 1].*

In accordance with Public Law 96-517, the contractor has elected to retain title to this invention. Inquiries concerning rights for its commercial use should be addressed to

Technology Reporting Office
JPL
Mail Stop 122-116
4800 Oak Grove Drive
Pasadena, CA 91109
(818) 354-2240

Refer to NPO-20425, volume and number of this NASA Tech Briefs *issue, and the page number.*

Solitons on WDM Beams in a Nonlinear Optical Fiber

This paper sets the ultimate limit on the maximum amount of optical data pulses that can be sent through a single fiber in a given period under the wavelength-division-multiplexed (WDM) format. The discovery in 1973 that optical soliton on a single wavelength beam can exist in fiber is one of the most significant events since the perfection of low-loss optical fiber communication. This means that, in principle, data pulses may be transmitted in a fiber without degradation forever. This soliton discovery sets the ultimate goal for optical fiber communication on a single-wavelength beam. Another most significant event is the development of WDM transmission in a single-mode fiber. This means that multiple beams of different wavelengths, each carrying its own data load, can propagate simultaneously in a single-mode fiber. This WDM technique provides dramatic increase in the bandwidth of a fiber. However, due to the presence of complex nonlinear co-propagating pulses on different wavelength beams, it is no longer certain that WDM soliton can exist. The existence of solitons is a blissful event in nature. It is a marvel that the delicate balance between the dispersion effect and the nonlinear effect can allow a specially shaped optical pulse to propagate in the fiber without degradation. They occur only on single-wavelength beams. When beams with different wavelengths co-propagate in a single-mode fiber, such as in the WDM case, interaction of pulses on different beams via the nonlinear cross-phase-modulation (CPM) effect (the Kerr effect) is usually instrumental in destroying the integrity of solitons on these wavelength multiplexed beams. This paper shows that temporal solitons can exist on WDM beams in a single fiber under appropriate conditions. The existence of these solitons critically depends on the presence of the nonlinear CPM effect of the WDM beams. Just as the earlier single-beam soliton case, this discovery sets the ultimate goal for optical fiber communication on WDM beams.

This work was done by Cavour Yeh and Larry Bergman of Caltech for **NASA's Jet Propulsion Laboratory**. *To obtain a copy of the report, "The Existence of Optical Solitons on Wavelength Division Multiplexed Beams in a Nonlinear Fiber," see TSP's [page 1].*

In accordance with Public Law 96-517, the contractor has elected to retain title to this invention. Inquiries concerning rights for its commercial use should be addressed to

Technology Reporting Office
JPL
Mail Stop 122-116
4800 Oak Grove Drive
Pasadena, CA 91109
(818) 354-2240

Refer to NPO-20772, volume and number of this NASA Tech Briefs *issue, and the page number.*

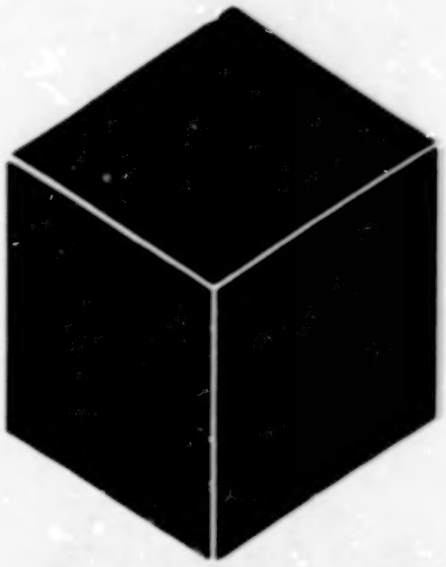

Materials

Hardware, Techniques, and Processes

29 Extended Shelf Life for PMR Polyimide Resins and Prepregs
30 Plasma CVD of Boron Carbide by Pulsed Secondary Discharge
30 Plasma-Sprayed Selective Emitters for Thermophotovoltaics

Books and Reports

31 Nesting-Hoop Solar Sail

BLANK PAGE

Extended Shelf Life for PMR Polyimide Resins and Prepregs

Secondary alcohols are used in place of primary alcohols.

John H. Glenn Research Center, Cleveland, Ohio

An improved class of formulations for PMR polyimide resins retards the imidization that undesirably occurs during handling and storage. While imidization is desired at the final (deliberate polymerization) stage of production of a polyimide, imidization results in premature aging when it occurs during earlier stages of synthesis, shipping, prepregging, and fabrication layup. By retarding imidization at storage and handling temperatures, the improved class of formulations increases both shelf life and the upper limit of allowable temperature for handling and storage prior to final polymerization.

The improved class of formulations is best explained with reference to the origin of the PMR concept: U.S. Patent 3,745,149, issued on July 10, 1973, disclosed that polyimides can be synthesized from mixtures of monomeric reactants that have been prepared by using lower (primary) alcohols (usually, ethanol or methanol) to esterify anhydride end caps and aromatic dianhydrides. The primary alcohols are also used as solvents for the reactants. A solution that incorporates such reactants plus an aromatic diamine in the mole ratio of [*N* diester diacid: *N*+1 diamine: 2 ester acid end cap] constitutes a monomeric mix which, at high temperature, polymerizes ("cures"), becoming a polyimide; hence, the evolution of the term "polymerization of monomeric reactants," now known better by its abbreviation, "PMR." Numerous variations of the basic PMR concept have been published since the original patent was issued, but, until now, none of these variations has departed from the use of primary alcohols to prepare methyl or ethyl ester acids.

The major disadvantages of conventional commercial PMR formulation and processing are limited shelf life at room temperature, short working life, and high sensitivity to temperature excursions above room temperature. These disadvantages are associated with premature imidization during all phases of PMR usage (synthesis, manufacturing, shipping, handling, storage, and fabrication). For example, typical commercial PMR-15 polyimide prepregs are out of manufacturing specification after a shelf life of only one to three weeks at room temperature. In many cases, the shelf life is even shorter for other PMR formulations, e.g., PMR-II-50. While PMR shelf life and working time can be extended by refrigeration and ensured by careful monitoring of temperature histories, this practice adds to the costs of PMR products.

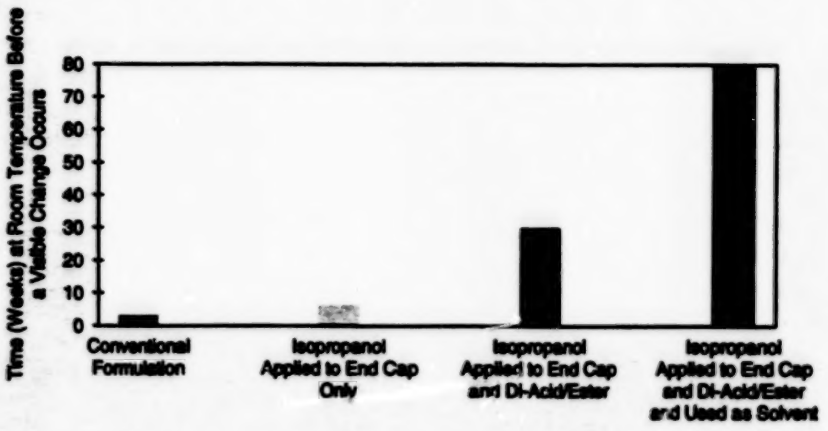

Shelf Lives of Four PMR-15 Solutions were measured. The solutions were products of four different formulations, ranging from the conventional formulation (primary alcohols used as esterification reagents and solvents) through partly conventional and partly improved formulation (isopropanol substituted for primary alcohols in some aspects) to totally improved formulation (isopropanol used exclusively as esterification reagent and solvent).

The improved class of formulations involves the use of secondary alcohols (usually, isopropanol) instead of primary alcohols for esterification of the anhydride end caps and dianhydride monomers and as solvents for the resulting isopropyl ester acids. In comparison with PMR resins made conventionally by use of primary alcohols, PMR resins made by use of isopropanol are less reactive at comparable storage or handling temperature, without changing typical imidization or curing temperatures. For example, PMR-15 resin made with isopropanol may be stored or handled at temperatures up to 50 °C higher than PMR-15 resin made with a primary alcohol (methanol) in order to produce comparable amounts of imide-aging products in both resins after equal handling and storage times.

This improvement affords a wide margin against mishandling of PMR solution, reducing or, in some cases, eliminating the need for refrigeration and monitoring of temperature histories. The results include not only increased shelf life (see figure) but also decreased costs of shipping and handling, more consistent processability, reduced variability among batches, improved hot-melt prepreg manufacturing, and reduced scrap rates. The improved formulations are also safer because in comparison with primary alcohols, isopropanol is less toxic and less flammable. Also, the longer retention time of isopropanol compared to methanol or ethanol during composite processing may be beneficial to some processing techniques, e.g., solvent-assisted resin transfer molding (SARTM) techniques.

This work was done by William B. Alston of the Army Research Laboratory; Daniel A. Scheiman of Dynacs Engineering, Inc.; and Gloria S. Sivko of **Glenn Research Center**. *Further information is contained in a TSP [see page 1].*

Inquiries concerning rights for the commercial use of this invention should be addressed to NASA Glenn Research Center, Commercial Technology Office, Attn: Steve Fedor, Mail Stop 4–8, 21000 Brookpark Road, Cleveland, Ohio 44135. Refer to LEW-16691.

Plasma CVD of Boron Carbide by Pulsed Secondary Discharge

Rates of deposition can be increased and internal stresses decreased.

John H. Glenn Research Center, Cleveland, Ohio

An improved method of plasma chemical-vapor deposition (CVD) of a thin film of boron carbide has been devised. Boron carbide is useful because it is hard, is electrically insulating, withstands high temperature, and resists chemical attack. Plasma CVD of boron carbide involves the thermal dissociation of feed gases BCl_3, CH_4, and H_2. Prior to the development of the improved method, it had been found that in plasma CVD, the rate of growth is enhanced when the deposition substrate is biased with a positive dc voltage, which gives rise to a secondary discharge. However, the applied dc voltage must be limited (1) so that the current drawn by the secondary discharge does not exceed the capacity of the bias power supply, and/or (2) the current drawn is not so large as to adversely affect the boron carbide deposit.

In the improved method, the bias potential is pulsed instead of steady. Taking advantage of the ability of a pulse circuit to sustain high voltage and the associated high current for a short time, pulses of bias potential higher than the limiting dc bias potential can be applied to the deposition substrate. The pulse-repetition frequency and duty cycle can be chosen so that for a given high potential, the time-averaged secondary-discharge current does not exceed the capability of the power supply or is not so high as to harm the deposit. For a given pulse-repetition frequency, one can trade applied potential versus duty cycle at the limiting time-averaged current; in other words, one can choose a potential as high as desired, as long as one makes the duty cycle short enough.

The beneficial effect of increasing the applied potential is attributed to a consequent increase in electron temperature. The higher the electron temperature, the greater the rate of dissociation of feed-gas molecules by impact of electrons.

During CVD of boron carbide and some other hard materials, part of the momentum of impinging ions becomes converted to internal stresses, which accumulate as the deposits grow. The buildup of internal stresses limits the maximum desirable thickness of a deposit in the sense that if one attempts to make the deposit thicker, the internal stresses are released through the formation of cracks. In the improved method, the peak potential, pulse-repetition frequency, and duty cycle can be regarded as process parameters that can be adjusted to prevent the formation of cracks: The magnitude of the bias defines the momentum and kinetic energy of the impinging ions, whereas the duty cycle and the pulse-repetition frequency define the time during which the deposited material can release some of its internal stresses.

This work was done by Joachim V. R. Heberlein and Olivier B. Postel of the University of Minnesota for **Glenn Research Center.**

Inquiries concerning rights for the commercial use of this invention should be addressed to NASA Glenn Research Center, Commercial Technology Office, Attn: Steve Fedor, Mail Stop 4–8, 21000 Brookpark Road, Cleveland, Ohio 44135. Refer to LEW-16716.

Plasma-Sprayed Selective Emitters for Thermophotovoltaics

Thin oxide films survive high temperatures and temperature gradients.

John H. Glenn Research Center, Cleveland, Ohio

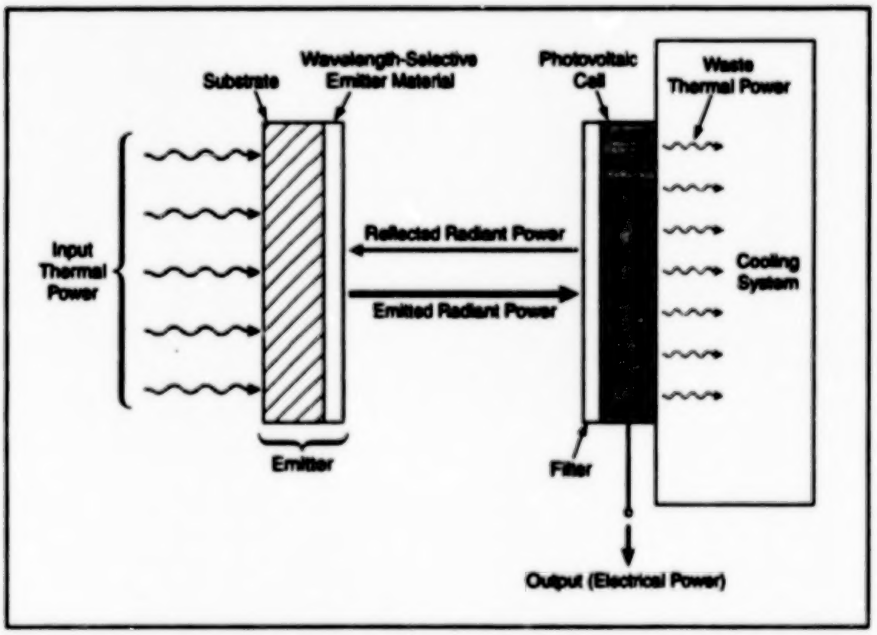

Figure 1. A Thermophotovoltaic Device is a thermal-to-electric power converter that includes a thermal emitter and a photovoltaic cell. A wavelength-selective emitter material and a short-wavelength-pass filter help to increase energy-conversion efficiency and reduce the cooling load for the cell.

Plasma spraying has been shown to be an effective means of depositing thin films of various oxides for use as wavelength-selective emitters for thermophotovoltaic devices (see Figure 1). Wavelength-selective emitters are needed to increase the overall efficiencies of such devices. A suitable emitter material for a given thermophotovoltaic device is one that, when heated to incandescence, emits light with a spectral peak or peaks that preferably lie within the wavelength band of peak response of the photovoltaic cell in the device; more specifically, what is desired is low emissivity at photon energies less than the band gap and high emissivity at photon energies above the band gap of the photovoltaic cell.

Oxides that have shown promise as wavelength-selective-emitter materials include some rare-earth oxides (erbia, thulia, and holmia, both singly and in combination), plus cobalt-doped spinel. Previous techniques for fabricating emitters of these and other materials include casting from

slurries and doping crystals with rare-earth oxides. The major disadvantage of cast emitters is mechanical weakness — especially the inability to withstand stresses caused by temperature gradients and thermal cycling. The major disadvantage of doped crystals is high cost.

To fabricate specimens for testing, the various oxide emitter materials were plasma-sprayed onto silicon carbide, alumina, and yttria substrates. Preparation of substrate surfaces by cleaning and roughening was found to be necessary to ensure adhesion and integrity of the deposited materials (see Figure 2). Some of the substrate surfaces were coated with reflective layers of refractory metals (platinum or rhodium) to suppress unwanted out-of-band radiation from the substrates. Emitter deposits with thicknesses from 15 to 250 μm were built up, a few microns per pass, by multiple passes of a plasma-spray apparatus.

The emitters (that is, the coated substrates) were tested in a bench-top thermophotovoltaic apparatus capable of reproducing prototypical operating conditions. The apparatus included an electrical heater for the emitter, and a 0.70-eV GaSb photovoltaic cell equipped with an integral filter. This apparatus was designed to enable the comparison of the cell output power, total power emitted, and conversion efficiency for various emitters under similar conditions.

In the tests, the plasma-sprayed emitter materials were found to retain their spectral emission characteristics through the deposition process. They were found to survive prototypical operating conditions, including temperatures up to 1,760 K and associated temperature gradients. The plasma-sprayed emitter materials did not exhibit any observable degradation during long-term operation at high temperature (3,600 hours at 1,500 K). Under the given test conditions, the best of the emitter materials tested was found to be a mixture of erbia and thulia; in comparison with a single oxide, the mixture provided stronger emission and hence more useful power within the wavelength band of the photovoltaic cell.

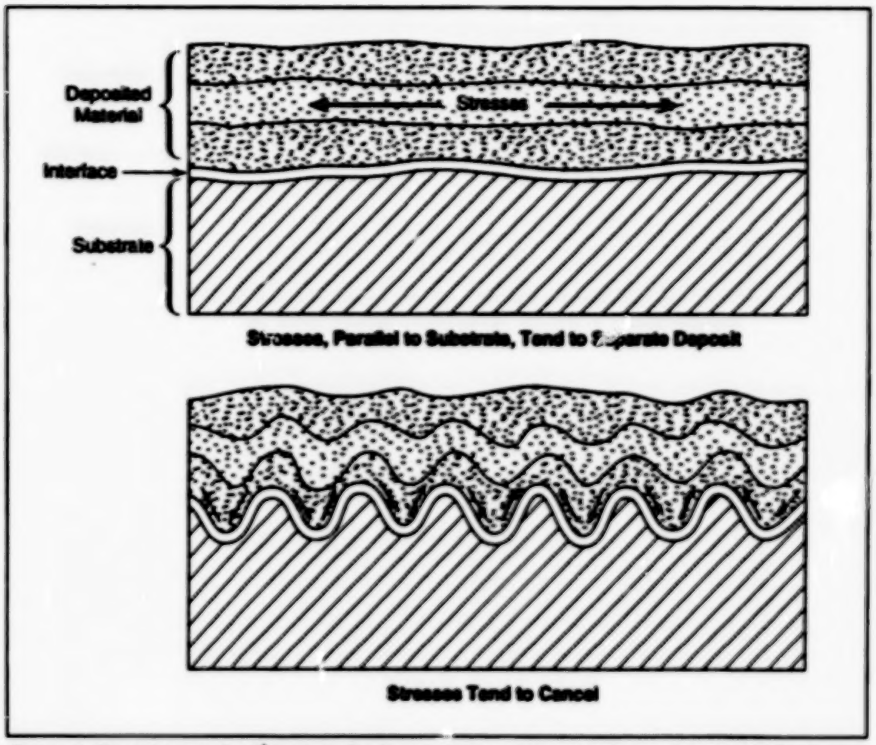

Figure 2. Roughening the Substrate Surface breaks up internal stresses, thereby helping to prevent delamination of the deposited material.

This work was done by Christopher J. Crowley and Nabil A. Elkouh of Creare, Inc., for **Glenn Research Center.**

Inquiries concerning rights for the commercial use of this invention should be addressed to NASA Glenn Research Center, Commercial Technology Office, Attn: Steve Fedor, Mail Stop 4–8, 21000 Brookpark Road, Cleveland, Ohio 44135. Refer to LEW-16809.

Books and Reports

Nesting-Hoop Solar Sail

A report discusses a proposed nesting-hoop solar sail that would be used to propel a spacecraft on a deep-space mission. The nesting-hoop design concept was chosen as one that would afford a desired combination of small mass and compact stowage during launch. The sail would include multiple disks, each comprising a thin fabric stretched over a hoop of wire or thin tubing (e.g., hypodermic-needle tubing). The adjacent hoops would be bonded together by springy extensions that would be fabricated in their sail-deployed positions. The sail would be stowed by folding at the springy extensions. Successive hoops would be progressively slightly smaller so that when stowed, the hoops would nest and therefore the thickness of the stowed sail would be approximately proportional to the thickness of the fabric (instead of the much greater thickness of the hoops). The fabric would not be folded for stowage; consequently, the spring tension (and thus the required thickness of the hoops) needed to keep the fabric from wrinkling could be kept to a minimum. The sail would be deployed by allowing it to unfold under its own springiness.

This work was done by Brian Wilcox of Caltech for **NASA's Jet Propulsion Laboratory.** *To obtain a copy of the report, "Nesting-Hoop Solar Sail," see TSP's [page 1].*
NPO-20879

BLANK PAGE

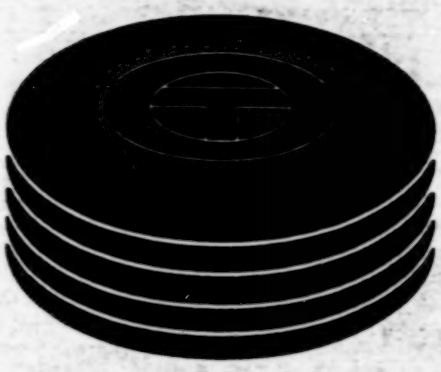

Computer Programs

Fabrication Technology

35 Software for Designing Plasma Reactors for Microelectronics

BLANK PAGE

Fabrication Technology

Software for Designing Plasma Reactors for Microelectronics

Outer-space plasmas and arc-jet plasmas are well known to many researchers at NASA. Efforts to understand the structures of these plasmas have consumed years of research at various NASA laboratories. Computational modeling of such plasmas involves analyses of multicomponent, multitemperature flows, and many computer codes developed by NASA are available for this purpose. Now, researchers at Ames Research Center have applied their expertise to understand a different kind of plasma — the kind used in manufacturing integrated circuits.

Typically, in such manufacturing, a weakly ionized plasma is used to etch fine patterns (smallest dimensions of the order of 10^{-7} m) in a silicon wafer. The discharge gas (the gas used to generate the plasma) could be chlorine or some type of fluorocarbon, depending on the material to be etched or the required functionality. The objective is to obtain a highly directional (even vertical) etched profile at a rapid rate, with minimum use of chemicals. If one were to use the chemicals in their liquid form — in what is known as "wet etching" — this objective would be compromised. Because chemical etches are "directionally blind," wet etching results in isotropic features. In contrast, dry etching with the help of a plasma achieves desired directionality through the combined action of reactive atoms or radicals and vertical bombardment of the surface with ions to clear off chemical-reaction products.

It is of interest to the microelectronics community to understand this dry process in order to optimize the process and design the right kind of reactor. That is where computational modeling is valuable. A computer code called Semiconductor Equipment Modeling Software (SEMS) has been developed to enable such modeling. This program solves equations of multicomponent, multitemperature, chemically reacting flows. The set of equations includes the Navier-Stokes equations of subsonic flow of gases, a gas-energy equation, an electron-energy equation, multicomponent conservation-of-chemical-species equations, and Maxwell's equations for determining the power coupled to the plasma from an inductive coil or other external power source.

The coupling of several such equations with disparate time scales results in a stiff (in the mathematical sense) problem. Time scaling of the equations has been explored in an effort to find ways to solve the problem rapidly. SEMS has been used to model commercial reactors and processes common in the fabrication of integrated circuits. Results have been obtained for nitrogen, chlorine, carbon tetrafluoride, and other plasmas in inductively coupled plasma reactors for processing 300-mm wafers in preparation for the next-generation circuits.

This program was written by Deepak Bose of Boret Thermosciences Institute and T. R. Govindan and M. Meyyappan of Ames Research Center. For further information, please contact M. Meyyappan at (650) 604-2616 or meyya@orbit.arc.nasa.gov.
ARC-14531

BLANK PAGE

Mechanics

Hardware, Techniques, and Processes

39 Differential-Pressure Relief Valve

39 Magnetic Couplings for Gas-Driven Catapults

BLANK PAGE

Differential-Pressure Relief Valve

Differential pressure between two fluids can be regulated without mixing them.

Lyndon B. Johnson Space Center, Houston, Texas

A relief valve has been designed to limit the differential pressure between two fluids that are not allowed to be mixed. This valve offers advantages over both simple check valves and simple relief valves. A simple relief valve vents a fluid at the preset absolute relief pressure, but offers no means for limiting the differential pressure between two fluids. A simple check valve can be used to limit the pressure between two fluids, but when the valve opens to relieve differential pressure, one fluid flows into the other one; thus, a simple check valve is not suitable for a system in which the two fluids must not be mixed.

The present valve (see figure) includes two pistons, one of which is spring-loaded and slides in response to the balance between the differential pressure and spring forces. The other piston rests against a hard stop provided by a socket-head cap screw, which is used to adjust the spring load and thus the differential-pressure relief setting. O-ring seals on the pistons prevent mixing and unintended venting of the fluids.

The lower-pressure fluid is deemed to be at the reference pressure and is connected via the uppermost (in the figure) port. The higher-pressure fluid is connected via the lowermost port. When the higher pressure exceeds the reference pressure by the preset amount, the piston moves upward, uncovering a vent hole and thus allowing excess higher-pressure fluid to escape without mixing with the lower-pressure fluid.

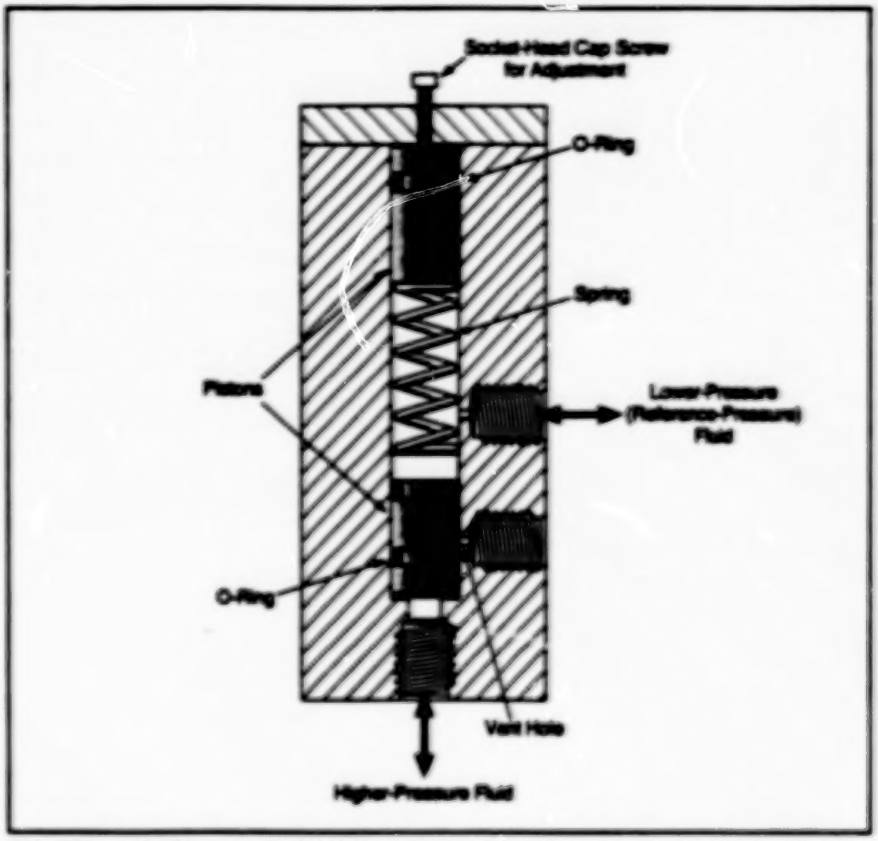

This Differential-Pressure Relief Valve vents the fluid that enters the lowermost port when its pressure exceeds the reference pressure by a preset amount. There is no mixing of the higher-pressure and lower-pressure fluids.

This work was done by Joseph Robert Trombley of Johnson Space Center and James Dwight Baker and James Everett Bryan of McDonnell Douglas Corp. Further information is contained in a TSP [see page 1].
MSC-22607

Magnetic Couplings for Gas-Driven Catapults

Projectiles would move along the outsides (instead of the insides) of launching tubes.

Marshall Space Flight Center, Alabama

A proposed magnetic-coupling scheme would afford additional degrees of freedom to optimize the designs of gas-driven catapults or launchers. The scheme could be applied to gas guns in diverse applications, including launching spacecraft or aircraft, propelling various objects at high speeds along the ground, and accelerating objects to high speeds for research on hypervelocity impacts.

Heretofore, the usual approach to designing a gas-driven launcher has involved designing a launching tube to accommodate the projectile; the rear end of the projectile would be configured as a piston, and pressurized gas would be introduced into the tube behind the piston to accelerate the projectile to the desired muzzle velocity. If the projectile is a spacecraft, aircraft, or other large object, then this approach entails major disadvantages in that the tube must be made very wide and the amount of pressurized gas that must be supplied is correspondingly large.

The proposed magnetic-coupling scheme would make it possible to launch a projectile by use of one or more launching tube(s) narrower than the projectile. Thus, one could design a launching system that would function with smaller amount of gas (albeit at a higher pressure needed to generate the required accelerating force over a smaller piston area). By making it possible to use a narrower tube or tubes, the proposed scheme would also make it possible or easier to design a staged compressed-gas system that would utilize

compressed gas and compression energy more efficiently.

This work was done by Glen A. Robertson of **Marshall Space Flight Center.**

This invention is owned by NASA, and a patent application has been filed. Inquiries concerning nonexclusive or exclusive license for its commercial development should be addressed to Sammy Nabors, MSFC Commercialization Assistance Lead, at (256) 544-5226 or sammy.nabors@msfc.nasa.gov. Refer to MFS-31184.

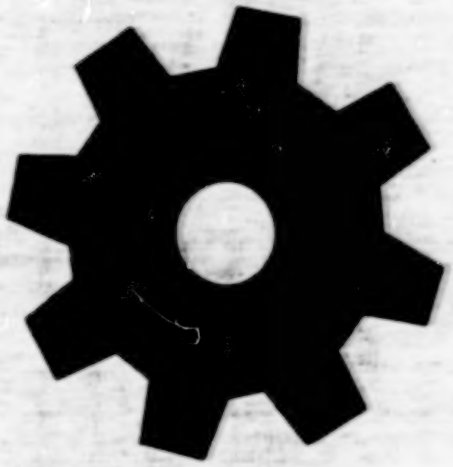

Machinery

Hardware, Techniques, and Processes

43 Compact, Recuperated, Binary-Fluid Rankine-Cycle Engine

44 Vortex-Fired Liquid-Fuel Rocket Combustion Chambers

44 Systems for Dynamic Control of Growth of Protein Crystals

42

BLANK PAGE

Compact, Recuperated, Binary-Fluid Rankine-Cycle Engine

The primary advantages of this engine are compactness and relatively high energy-conversion efficiency.

John H. Glenn Research Center, Cleveland, Ohio

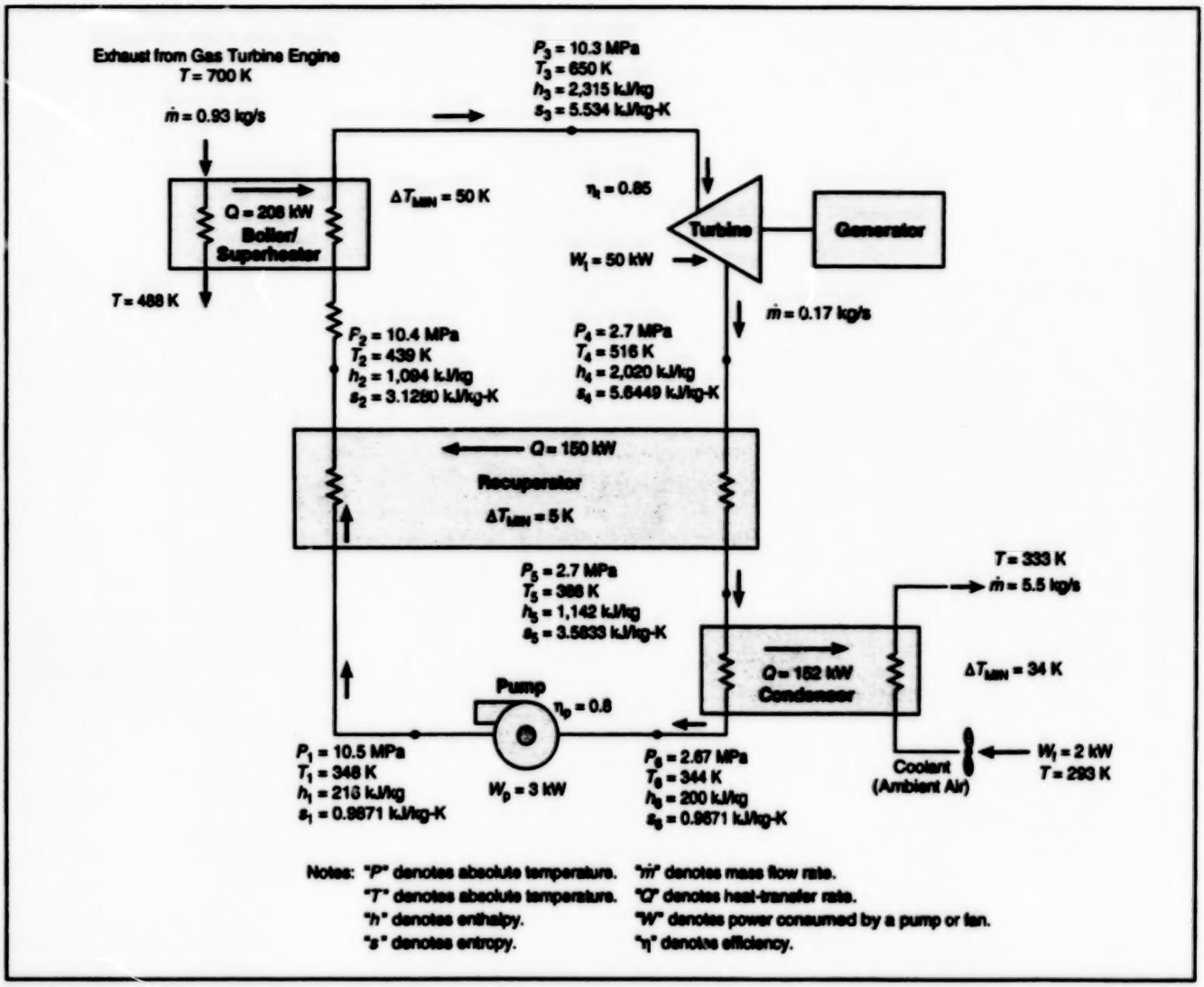

This Recuperated, Binary-Fluid Rankine-Cycle Engine exploits the unique characteristics of a binary working fluid to recycle some of the heat that would otherwise be dumped out through the condenser. This improves the system efficiency and reduces its size. The thermodynamic parameters indicated in the figure were calculated for a working fluid of 80 weight percent ammonia and 20 weight percent water.

A Rankine-cycle engine that contains a binary working fluid (ammonia + water) and a recuperative heat exchanger has been built and tested. This engine is a prototype of "bottoming"-cycle engines that would be used to extract additional useful power from the exhaust heat of gas turbine engines. Its advantages are well suited to vehicles, where volume and weight are important constraints.

The described binary-fluid Rankine cycle has higher efficiency and smaller volume than Rankine cycles with single-component working fluids. It has nearly the same efficiency but much smaller volume than the binary-fluid Kalina Rankine cycle, which entails the use of separators and additional heat exchangers to vary the proportions of ammonia and water in the working fluid at various points in the cycle. The present cycle does not vary the composition of the working fluid. Because the separators and additional heat exchangers are not needed, an engine based on the present recuperated, binary-fluid Rankine cycle has only a fraction of the volume of the corresponding Kalina-cycle system.

The present recuperated, binary-fluid, Rankine-cycle engine (see figure) includes a boiler/superheater, a turbine that drives an electric-power generator, a condenser, a pump, and a recuperative heat exchanger ("recuperator" for short). The boiler/superheater transfers heat from the gas-turbine exhaust or other source to the working fluid. The turbine extracts useful power from the heat in the working fluid. The condenser removes the final waste heat that is of too low a temperature to be worth recovering. The recuperative heat exchanger transfers heat from the turbine-outlet/condenser-inlet junction (a higher-temperature, lower-pressure location) to the pump-outlet/boiler-inlet junction (a lower-temperature, higher-pressure location). In so doing, the recuperator recycles some of the heat that would otherwise be dumped out through the condenser as waste heat; thus, the main effect of the recuperator is to increase the energy-conversion efficiency.

A large variation (≈100 K) in the saturation temperature of the ammonia/water mixture with the vapor fraction during boiling makes recuperation possible in

this cycle. In designing the recuperator, one must consider the details of heat transfer and the behavior of the binary working fluid. The flow on the low-temperature side of the recuperator proceeds through the sequence of single-phase liquid, two-phase boiling, and superheated vapor. On the high-temperature side of the recuperator, the flows at the corresponding positions in the recuperator may be two-phase condensing or superheated vapor. Thus, the operation of the recuperator entails several different two-phase heat-transfer phenomena, all of which must be taken into account.

Both theoretical calculations and experiments have shown that this recuperated, binary-fluid Rankine-cycle engine operates with energy-conversion efficiency 1.5 or 2.0 times that of an otherwise identical engine that contains either ammonia (only) or water (only) as the working fluid. It has also been found that the total volume of the three heat exchangers (the boiler/superheater, the condenser, and the recuperator) in this engine is 10 percent less than the total volume of the two heat exchangers (the boiler/superheater and the condenser) for a nonrecuperated engine using the binary fluid at the same source and sink temperatures.

This work was done by Christopher J. Crowley and Martin A. Shimko of Creare, Inc., for **Glenn Research Center.**

Inquiries concerning rights for the commercial use of this invention should be addressed to NASA Glenn Research Center, Commercial Technology Office, Attn: Steve Fedor, Mail Stop 4–8, 21000 Brookpark Road, Cleveland, Ohio 44135. Refer to LEW-16834.

Vortex-Fired Liquid-Fuel Rocket Combustion Chambers

Swirling cold propellants and pressure gradients keep hot gases away from walls.

Marshall Space Flight Center, Alabama

Liquid-fuel rocket engines that utilize vortex flow fields to keep combustion-chamber walls cool have been investigated in computational simulations and experiments. In an engine of this type, the vortex flow establishes radial gradients of pressure and density that cause the lower-density hot combustion products to be confined near the central axis of the combustion chamber while cold gases yet to be burned are centrifuged to the combustion-chamber wall. Keeping combustion-chamber walls cool in this manner reduces or eliminates damage by heat and oxidation, thereby (1) eliminating the need for leak-prone cooling passages, (2) extending the operational lifetimes of combustion chambers, and (3) creating an opportunity to fabricate combustion-chamber walls more easily, using relatively inexpensive materials (possibly even lightweight composite materials) instead of expensive alloys.

For the most part, the combustion chamber in an engine of this type has a conventional appearance: it includes a head-end dome, a barrel section, and a section that converges from the barrel to a throat that opens into an expansion bell. A vortex flow field with a co-swirling, counter-flowing character is produced in the following way: One of the propellants (typically, oxygen at supercritical pressure) is injected circumferentially tangential through ports just forward of the junction between the barrel and the section that converges to the throat. The other propellant (typically, liquid hydrogen) is injected either from the head end or through a porous liner in the chamber wall.

The circumferential component of the injection flow forms a free vortex that spirals forward along the wall of the barrel to head end, where it turns inward to form a second vortex, concentrated along the axis, that flows out of the chamber at the aft end. If the fuel is fed through the wall, the upwelling oxygen burns the incoming fuel and carries it forward and into the axial vortex. If the fuel is injected from the head end, then it burns only along the axis. In both fuel-injection schemes, the radial gradients of pressure and density prevent hot combustion products from migrating out to the wall. Instead, the hot gases are buoyed toward the axis. Thus, the wall stays cool.

The propellant injectors can be relatively simple because unlike in other rocket engines, there is no need to atomize or mix the propellant fluids immediately upon injection. All of the necessary atomization and mixing is effected by the coaxial vortex flow. Yet another advantage of engines of this type is that they appear to be immune to combustion instability.

This work was done by William H. Knuth, Martin Chiaverini, and Daniel J. Gramer of Orbital Technologies Corp. for **Marshall Space Flight Center.** *For further information, please contact the company at knuthw@orbitec.com*

In accordance with Public Law 96-517, the contractor has elected to retain title to this invention. Inquiries concerning rights for its commercial use should be addressed to

Orbital Technologies Corporation
1212 Fourier Drive
Madison, WI 53717

Refer to MFS-31477, volume and number of this NASA Tech Briefs *issue, and the page number.*

Systems for Dynamic Control of Growth of Protein Crystals

Key parameters that affect crystallization can be monitored and controlled.

Marshall Space Flight Center, Alabama

Computer-controlled laboratory apparatuses for real-time monitoring and control of the growth of protein crystals are undergoing development. By use of an apparatus of this type, one can monitor and control several parameters that affect the growth of protein crystals; these parameters include temperature, pH, ionic strength, concentration of solute, rate of change of concentration of solute, and possibly others. One can utilize the monitoring capabilities to make decisions on the basis of the measured parameters. One can utilize the control capabilities to effect precise control of growth; one can also start, stop, or reverse growth at will.

In a representative apparatus of this type, precipitating solutions are mixed in a plastic crystallization chamber. The apparatus includes two syringes connected to the crystallization chamber via plastic tubes. By use of a stepping motor that drives a shuttle, the plunger of one syringe is driven in the emptying direction, while the plunger of

the other syringe is driven in the filling direction. Probes to monitor electrical conductivity (as an indication of concentration), pH, ionic strength, and temperature are incorporated into the crystallization chamber. Temperature can be controlled by use of a Peltier-effect (thermoelectric) incubator unit. Electronic circuits for controlling the motor, controlling the temperature, and converting the probe outputs into a digital form readable by the associated computer are contained on a printed-circuit board.

An apparatus of this type can be assembled in building-block fashion: Optionally, it can be constructed without the probes and associated circuitry, which can be added later. Another conceptual variation of the basic design would be a multiplexing design in which multiple syringes, multiple motor drives, and/or a manifold and valves would be used to control flows to multiple crystallization chambers so as to test multiple values of molarity and multiple rates of change of molarity of the crystallizing protein.

This work was done by Leonard Arnowitz and Emanuel Steinberg of BioSpace International, Inc., for **Marshall Space Flight Center**. *For further information, please contact the company at bsi@biospace11.com.*

In accordance with Public Law 96-517, the contractor has elected to retain title to this invention. Inquiries concerning rights for its commercial use should be addressed to

BioSpace International, Inc.
Attn. Leonard Arnowitz, President
4701 Willard Ave., Suite 1236
Chevy Chase, MD 20815

Refer to MFS-31400, volume and number of this NASA Tech Briefs *issue, and the page number.*

BLANK PAGE

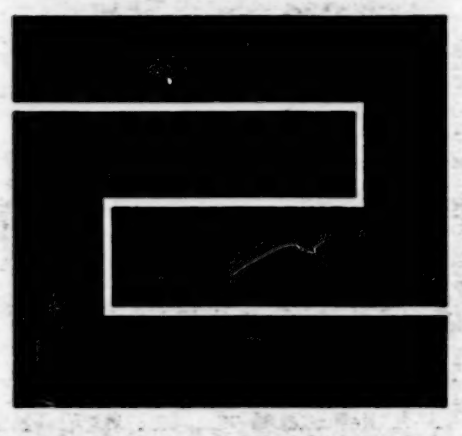

Fabrication Technology

Hardware, Techniques, and Processes

49 Writing Circuit Patterns by Use of Scanning UV Lasers

BLANK PAGE

Writing Circuit Patterns by Use of Scanning UV Lasers

Prototype circuits can be fabricated rapidly.

NASA's Jet Propulsion Laboratory, Pasadena, California

Scanning ultraviolet (UV) lasers would be used to expose ultraviolet-sensitive photoresists to form patterns of conductors for electronic circuits, according to a proposal. Heretofore, such patterns have been formed by exposing photoresists to collimated ultraviolet or visible light through contact or proximity photomasks. The use of scanning lasers would make it unnecessary to make or use masks, and it would be amenable to rapid fabrication of prototype circuits.

In forming a given circuit pattern, the scanning of the ultraviolet laser would be controlled by use of the same plotting data, generated by computer-aided-design software, that would otherwise have been used to plot the photomask for the pattern. In the case of a negative photoresist, the portion of the resist not exposed to the laser would be removed by a stripping compound after the photoresist had been developed. The metal underlying the exposed and stripped areas would be etched away. Then the remaining exposed photoresist would be stripped away.

In the case of a positive photoresist covering a very thin chromium-coated medium (insulating substrate), the part of the resist exposed by the laser would be removed by developing and stripping, then through the resulting openings in the resist, the desired electrically conductive material (typically, copper or gold) would be electrodeposited through the openings in the resist. Finally the unexposed resist and the thin chromium coat would be stripped from the medium.

This work was by Frank Hartley and Steve Bolin of Caltech for **NASA's Jet Propulsion Laboratory**. *Further information is contained in a TSP [see page 1].*
NPO-20495

BLANK PAGE

Mathematics and Information Sciences

Hardware, Techniques, and Processes

53 Algorithm for Calibrating an Imaging Interferometer
54 Software Collects Planning and Scheduling Requirements
54 Software for Ground Processing of Data From Landsat 7

Books and Reports

55 Fast Observers for Spacecraft Pointing Control

BLANK PAGE

Algorithm for Calibrating an Imaging Interferometer

Conventional "flat-field" calibration is obviated and systematic noise is reduced.

Ames Research Center, Moffett Field, California

An algorithm has been devised to greatly simplify and improve the calibration and the reduction of systematic noise of an imaging interferometer or other similar interferometric instrument. Prior to the advent of this algorithm, such calibration was achieved by means of a conventional "flat-field" correction method that requires uniform illumination of all pixels in the image detector of the instrument. To achieve uniform illumination, it is often necessary to disassemble the instrument to separate the image detector from the instrument optics, taking care to keep all optical and electronic components clean and to restore the original optical alignment upon reassembly.

This algorithm makes it unnecessary to illuminate the detector uniformly or to perform difficult and time-consuming laboratory calibration, disassembly, and reassembly procedures. Calibration information can be extracted from ordinary images — even from highly variable scenes. With this algorithm, calibration can be performed with much more flexibility — in the laboratory or in the field. Moreover, the algorithm makes it possible to calibrate the instrument in nearly real time — immediately before or after acquisition of interferometric images — so that one can have some assurance that there has not been enough time for vibrations and other environmental factors to affect the calibration significantly.

Imaging interferometers for which this algorithm was designed acquire a spectral image one spatial line at a time on an image detector that contains a two-dimensional pixel array. In contrast to a conventional scanning interferometer, the optics in this imaging interferometer are fixed. The array is illuminated by two beams of light that interfere coherently, giving rise to an interferogram. The interferograms are recorded, then Fourier-transformed to obtain spectra.

The optical configuration of the instrument is such that each pixel along one dimension represents an increment of position along the spatial line, while each pixel along the perpendicular dimension represents an increment of the path-difference between the two interfering beams at that position. The data product of the interferometer, obtained by putting together the spatial and Fourier-transform spectral information from all spatial lines across a scene, is an image "cube" that comprises a two-dimensional spatial image with an inverse Fourier transform of a spectrum for each spatial pixel.

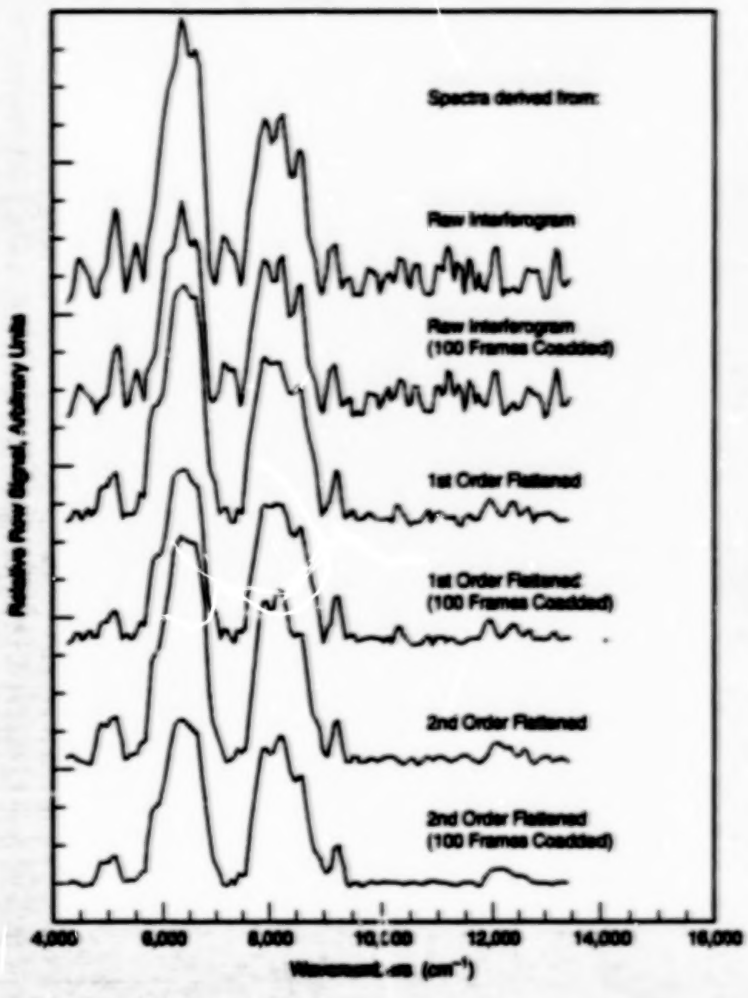

The Results After Various Stages of Processing are shown for a particular interferogram row of a detector array. The plot shows corresponding spectra of the interferograms after Fourier transformation.

The present calibration algorithm exploits the special physical and mathematical characteristics of the two-beam interference phenomenon (i.e., constraints and symmetry properties), as rendered by the optics of the instrument onto the detector plane. The spatial and interferogram coordinates at the detector plane are orthogonal and thus separable. Thus in principle, a single frame observation that is uniform along the spatial coordinate (or an average of many frames that approaches such uniformity) will yield fringes of equal inclination and that are parallel or unvarying along the spatial coordinate. The algorithm transforms real, imperfect fringe patterns so that they can be represented as fringes of equal inclination, enabling a very effective extraction of systematic noise for subsequent use in treating data cubes on a frame-by-frame basis.

The algorithm prescribes a series of reversible transformations to the two-dimensional Fourier domain of the pixel-array space. An important part of the algorithm is a row-wise-phase-alignment subalgorithm that is analogous to the formalism used to process asymmetrical interferograms produced by scanning Fourier spectrometers. Phase alignment eliminates the effects of variation in interference-fringe path-difference scales over rows of the detector plane. The resulting signal in Fourier space then represents the spectrum of the row-wise coherently coadded interferograms of an entire

frame, is highly localized, and is optimally isolated from noise and systematic errors. The signal is filtered out, then an inverse composite transformation is performed to obtain a pixel-variation frame that is used to treat the image data.

The algorithm does not depend on such instrument parameters as the spatial and spectral ranges and resolutions. Additionally, the algorithm treats bad detector pixels in a self-consistent manner, and aberrations caused by imperfections in the detector and associated optics are accommodated. Image data treated by the algorithm approach the fundamental limit (defined by photon shot noise or random detector noise) of the signal-to-noise capability of the instrument. The benefits obtained from applying the algorithm to typical radiative spectra of the atmosphere are designated as "2nd order flattened" in the figure.

The algorithm has been implemented in prototype software that includes parts in Interactive Data Language (IDL) together with a comprehensive set of routines for processing imaging-interferometer-type data. It should be possible to make a commercially viable software product by translating the IDL code into an efficient computing language and integrating it with a comprehensive data-processing-and-visualization program that includes a user interface.

This work was done by Philip D. Hammer of **Ames Research Center.** *Further information is contained in a TSP [see page 1].*

This invention has been patented by NASA (U.S. Patent No. 5,675,513). Inquiries concerning nonexclusive or exclusive license for its commercial development should be addressed to the Patent Counsel, Ames Research Center, (650) 604-5104. Refer to ARC-14054.

Software Collects Planning and Scheduling Requirements

Configuration control is maintained, even as diverse users enter their data at will.

Marshall Space Flight Center, Alabama

Interim User's Requirements Collection (IURC) is a software system that generates an interactive graphical user interface that enables users of the International Space Station (ISS) to specify their payload-planning and -scheduling requirements via the World Wide Web (WWW). IURC includes (1) a Java applet that is dynamically distributed via the WWW and (2) four application programs that run on a dedicated host computer with a web server at Marshall Space Flight Center (MSFC).

The need for a system like IURC to collect ISS payload planning and scheduling requirements arises from several causes. The requirements are complex, lengthy, and diverse. The scarcity of Space Station resources causes significant competition for resources among experiments. In order to be able to perform its scheduling task, the Payload Operations Integration Center at MSFC needs a concise and comprehensive description of payload requirements (to ensure a valid schedule) and a good description of the payload flexibilities (to provide for effective utilization of available resources). In addition, the continuous operation of the ISS, the wide geographic dispersion of ISS users, and budgetary pressure to employ fewer operational personnel have made it necessary to seek an inexpensive solution in the form of software.

IURC incorporates three distinct innovations that synergistically ensure effectiveness in the collection of planning and scheduling requirements, with the needed fidelity and convenience, and at a cost less than the costs of other methods. These innovations are the following:

- The major innovation is a provision for graphical specification of requirements. IURC does more than merely use graphics to depict or interpret data entered via tables or forms; the graphical user interface is the data-entry mechanism.
- IURC provides "just-in-time" configuration control that is not visible to users. Configuration control begins when a user says that a set of data is ready to go; at this point, IURC makes a copy of the set of data. Users who enter data never see any effect of configuration control. Their data are not "locked," so that users never need to request that the data be "unlocked." Users are free to edit their data at will. However, the copies of data that users have designated as being ready to go and that are being used to produce ISS time lines are under full configuration control.
- The WWW implementation enables a user to interact with the system via a personal computer from any location. All data are kept on the web server at MSFC; except for entering data as described above, users never move, send, or track their data. In addition, by utilizing the combination of (1) a universally installed web browser and (2) the dynamically downloaded JAVA applet, IURC eliminates the need for users to install any software, yet is globally available to users.

This work was done by John Jaap and Elizabeth Davis of **Marshall Space Flight Center.** *For further information, please contact the MSFC Software Release Authority at (256) 544-7175.*

MFS-31416

Software for Ground Processing of Data From Landsat 7

This software generates archival data products and performs calibrations.

Goddard Space Flight Center, Greenbelt, Maryland

Three computer programs have been developed for ground processing of Enhanced Thematic Mapper Plus (ETM+) data from Landsat 7. The three programs and their functions are the following:

- The Landsat Processing System (LPS) program processes the Landsat 7 ETM+ data received by the Landsat ground station into an archival data product.
- The Image Assessment System (IAS) program assesses the quality of ETM+ data and performs calibration of the ETM+.
- The Level 1 Product Generation System (LPGS) program generates level-1 ETM+ digital image data products (this means that LPGS performs radiometric and geometric corrections of ETM+ digital image data).

This software differs from the software used to process data from older satellites of the Landsat series. The content and format

of the Landsat 7 wide-band (X-band) data stream are unique to the Landsat 7 system. While the data acquired by the Thematic Mapper sensors aboard the Landsat 4 and Landsat 5 satellites are similar to the ETM+ data, the ETM+ data stream received at the ground station is significantly different, such that the ground data-processing software developed for the older Landsat satellites cannot be used for ground processing of Landsat 7 data. Hence, it was necessary to develop the present three programs to handle the Landsat 7 ETM+ data.

A major difference between Landsat 7 and the older Landsat satellites is that Landsat 7 incorporates new radiometric calibration sources. The IAS program, in particular, implements new procedures for exploiting ETM+ observations of these sources for radiometric calibration.

The IAS source code is original. Large portions of the IAS source code were reused in developing the LPGS program.

The IAS program includes commercial-off-the-shelf software [Oracle for a data base and IDL for some digital image analyses], but these commercial programs are not embedded in the version of the IAS source code that the authors intend to distribute.

The software consists of lines of source code written principally in the C programming language and accompanied by descriptive documentation. The software is designed exclusively to run on the computer systems of the U.S. Landsat 7 ground data processing system, developed under management of the NASA Goddard Space Flight Center and delivered to the Earth Resources Observation System (EROS) Data Center of the U.S. Geological Survey for use during operations in orbit.

The Landsat 7 satellite is expected to transmit ETM+ data to a number (circa 10) of ground stations distributed around the globe. The stations are expected to be operated by international cooperators (foreign governments or government consortia) that will pay license fees to the U.S. Geological Survey. The LPGS, IAS, and LPGS source code will be of greatest interest to those involved in the development of the ground data processing systems for international cooperators. Other organizations interested in creating data products derived from ETM+ data for their customers may also be interested in this software.

This work was done by Robert J. Menrad of **Goddard Space Flight Center**, *Mina Samii of Computer Sciences Corp., and R. J. Thompson of the U.S. Geological Survey.*
GSC-14244

Books and Reports

Fast Observers for Spacecraft Pointing Control

A report discusses the design of fast stochastic observers for spacecraft pointing control. In this special context, "observers" signifies mathematical algorithms, implemented on computers aboard spacecraft, through which one processes sensory data (principally, the outputs of star trackers and gyroscopes) to estimate the states (attitudes and angular velocities) of the spacecraft. The development in the report was motivated by the presence of an attitude-dependent bias error in the star-tracker measurement associated with NASA's upcoming SIRTF (Space Infra-Red Telescope Facility) space telescope. This attitude-dependent bias term lies outside of basic linear estimation assumption, and the well-established Kalman theory is no longer optimal. The attitude-dependent bias term forces a step response through the dynamics of the onboard estimator each time the spacecraft is repositioned. If an optimal Kalman filter were used, its sluggish dynamics would create a long undesirable lingering output drift in the pointing response. While this drift error is small (e.g., at the arc-second level) it cannot be ignored for space telescope applications, and is the main reason that Kalman filters are routinely replaced by simple observers on important missions with stringent pointing requirements such as the Hubble Space Telescope and SIRTF.

In this report, a theoretical analysis of an attitude estimator comprising three decoupled single-axis observers leads to a globally optimal solution for designing a constrained stochastic observer of second-order form. This stochastic observer minimizes the variance of the attitude estimate, subject to a constraint that its poles lie to the left of a specified vertical line in the complex Laplace-transform s-plane. This so-called "fast observer" design allows the step response of the onboard estimator to be sped up with minimal degradation in the variance of the state estimate. Examples are presented to illustrate the optimal tradeoff between observer speed and estimation error.

This work was done by David S. Bayard of Caltech for **NASA's Jet Propulsion Laboratory**. *To obtain a copy of the report, "Fast Observers for Space Telescope Pointing Control with Application to SIRTF," see TSP's [page 1].*
NPO-20883

BLANK PAGE

Life Sciences

Hardware, Techniques, and Processes

59 *In Situ* Activation of Microencapsulated Drugs

BLANK PAGE

In Situ Activation of Microencapsulated Drugs

Activation could be effected by thermal, electromagnetic, ultrasonic, and/or other forms of energy.

Lyndon B. Johnson Space Center, Houston, Texas

In a new method of delivering drugs to target sites in a human body, (1) the drugs would be stored in inactive forms in timed-release microcapsules that would be injected, then (2) the drugs would be activated by exposing the target sites to suitable forms of penetrating energy that could include electromagnetic radiation (radio waves, light, or x rays), ultrasound, or heat, then (3) the drugs would diffuse out of the microcapsules. The method would be well suited for drugs that have short shelf lives in their active forms and/or could be activated at target sites upon exposure to nonharmful activation energy.

The concept of microencapsulation of drugs was reported in "Microencapsulation of Multiple Drugs" (MSC-22489), *NASA Tech Briefs*, Vol. 20, No. 11 (November 1996), page 92. To recapitulate: microcapsules are formed as multilammelar, multiple-immiscible-phase structures that include alternating hydrophilic and hydrophobic liquid layers surrounded by flexible, semipermeable, polymeric outer membranes. The skins are designed to allow sustained diffusion of the bioactive drugs out of the microcapsules.

The disadvantage of conventional liposomes and of previously developed microcapsule drug-delivery systems is that they are impractical for delivery of drugs that are chemically labile or that have short shelf lives in their bioactive forms. Typically, a liposome or a previously developed microcapsule does not contain both a drug precursor and activator; consequently, the contents of the microcapsule cannot be converted to the active form of the drug immediately before or after administration to the patient. Also, conventional microcapsules cannot be lysed *in situ* to release bioactive drugs at target tissue sites without deposition of large amounts of energy that could adversely affect the tissues.

A microcapsule for use in the proposed method (see figure) would include a spherical drug-permeable outer membrane that would enclose immiscible fluid compartments containing the drug precursor in one phase and an activating agent in another phase. The activating agent would be a substance that could be activated by one of the forms of energy mentioned above and that would, in turn, react with the drug precursor to produce the active form of the drug. Such microcapsules would have to be protected from the activating form of energy during storage and until the time of administration to a patient.

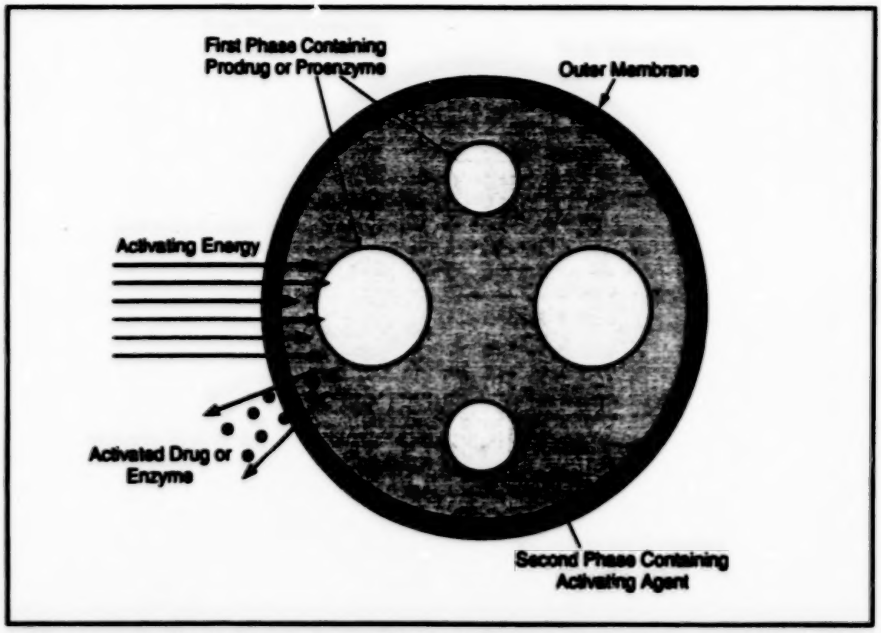

A Microcapsule Would Contain Immiscible Liquid Phases, the first phase consisting of spheroids containing a prodrug or a proenzyme, the second phase being the surrounding liquid containing an activating agent. Exposure to electromagnetic or ultrasonic energy would cause activation, after which the drug would diffuse through outer membrane to act on surrounding tissues.

Depending on the depth of the target site in the patient's body, the activating energy could be delivered from a transducer on the outside or, if necessary, from the inside by use of a catheter that contains a fiber-optic probe, ultrasonic or electromagnetic transducer, or other device. In a variation of the basic concept, the activating energy could also be utilized to stir the precursor and activator liquid phases together. In another variation, the activating agent could be contained within a thermosensitive membrane that could be ruptured to release the activating agent. Numerous other variations can readily be envisioned.

This work was done by Dennis R. Morrison of Johnson Space Center and Benjamin Mosier of Institute for Research, Inc. Further information is contained in a TSP [see page 1].

This invention is owned by NASA, and a patent application has been filed. Inquiries concerning nonexclusive or exclusive license for its commercial development should be addressed to the Patent Counsel, Johnson Space Center, (281) 483-0837. Refer to MSC-22866.

END

11-5-02